

Project Number: BJSQA12

GAIT ANALYSIS AND SPINAL ROTATION

A Major Qualifying Project Report:

Submitted to the Faculty

Of the

WORCESTER POLYTECHNIC INSTITUTE

In partial fulfillment of the requirements for the

Degree of Bachelor of Science

By

Michael Boucher

David Pierre

Savonne Setalsingh

Richard Wingert

Date: April 2012

Approved:



Prof. Brian J. Savilonis, Major Advisor

Acknowledgments

The group would like to thank the following people for their support and guidance throughout our Major Qualifying Project, without them the project wouldn't have progressed in the same manner. Thank you to Professor Brian J. Sivilonis, Adriana Hera, Thomas Fontecchio, James Monaco and the BME and ME department respectively.

Abstract

Understanding how the muscles and forces during the gait cycle are affected when different running techniques are used is an area of interest for many athletes, coaches, and physical therapists. This study looks to find a correlation between the effects of spinal rotation and the impact forces on the feet and knees while jogging. For a group of 40 runners, two force transducers were placed in the right insole of their shoe to measure the vertical forces upon landing during heel strike and a spinal rotation device was placed on their backs to measure spinal rotation. The forces were correlated to amount of spinal rotation during a jog with normal form, an exaggerated spinal rotation and a restricted spinal rotation. Musculoskeletal models of the knee and foot along with dynamic equations were used to solve for the forces in the appropriate muscles and bones. It was expected to see the initial contact force and the calculated knee loads decrease with greater rotation of the spine. The results showed there was no correlation to the reduction of force as a direct result of increased or decreased spinal rotation.

Table of Contents

Acknowledgments	2
Abstract.....	3
Table of Figures.....	8
Table of Tables.....	10
Executive Summary	11
1. Introduction	13
2. Background	15
2.1 The History of Gait Analysis	15
2.2 The Gait Cycle	19
2.2.1 Walking	19
2.2.2 Running.....	20
2.2.3 Alternative Running Styles.....	21
2.3 Injuries	21
2.3.1 Achilles Tendinitis	21
2.3.2 Shin Splints.....	22
2.3.3 Runners Foot Injuries.....	23
3. Instrumentation and Devices.....	25
3.1 Accelerometers.....	25
3.2 Potentiometer.....	26
3.3 Video Analysis	26
4. Project Strategy	28
4.1 Problem Statement.....	28
4.2 Objectives	28
4.3 Constraints.....	29
4.4 Functions/Specifications.....	30

5. Alternative Designs	31
5.1 Foot Transducer Component	31
5.1.1 Design 1.....	31
5.1.2 Design 2.....	31
5.1.3 Design 3.....	32
5.2 Spinal Rotation Component.....	32
5.2.1 Design 1.....	32
5.2.2 Design 2.....	32
6. Final Design	34
6.1 The Force Transducer System.....	34
6.2 Spinal Rotation System	34
6.3 Alterations to the Final Design	35
6.3.1 Dowel Length	35
6.3.2 Number of Force Transducers	36
6.3.3 Placement of Force Transducers	36
6.3.4 On/Off Switch	37
6.3.5 Connection of Potentiometer to the Dowels	37
6.3.6 Cover to Potentiometer	37
6.3.7 Back Plates	38
6.3.8 Velcro Fastenings.....	38
6.3.9 Data Acquisition Box Protection	38
6.3.10 Assembly.....	39
6.4 The Circuitry/Data Recording System.....	40
6.4.1 Assembly	43
7. Methodology.....	56
7.1 Force Transducers.....	56

7.2 Spinal Rotation.....	57
7.3 Video Analysis.....	58
7.4 Testing Procedure.....	59
7.5 Potentiometer.....	62
7.5.1 Tools used.....	62
7.5.2 Process.....	63
7.6 Force Transducer Calibration.....	65
8. Results.....	67
8.1 Force Transducer and Spinal Rotation Results.....	67
8.2 Video Results.....	69
8.2.1 Tracking.....	69
8.2.2 Force and Knee Analysis.....	69
8.3 Force Plate Results.....	71
9. Analysis.....	75
9.1 Voltage Output Analysis.....	75
9.1.1 Force Transducer Output.....	76
9.1.2 Spinal Output.....	78
9.2 Video Analysis.....	78
9.3 Force Plate Analysis.....	86
10. Discussion and Conclusion.....	87
11. Manufacturing.....	88
Works Cited.....	89
Appendix A.....	90
Appendix B.....	92
Appendix C.....	94
Appendix D.....	95

Appendix E	96
Appendix F	97
Appendix G.....	98
Appendix H.....	102
Appendix I	103

Table of Figures

Figure 1: Illustration from Borelli's book on the movement of animals depicting his biomechanical analysis of a man on his toes of one foot bearing a load (Baker, 2007).....	16
Figure 2: A subject of Braune and Fischer's wearing an experimental suit (Braun, 1992).....	18
Figure 3: A breakdown of the human gait cycle and how weight is transferred from stance phase to swing phase. HS represents heel strike and TO represents toe off (Pribut, 2010).	20
Figure 4: Spinal Rotation Device with Fanny Pack and Force Transducers on Insole.....	40
Figure 5: A schematic for the potentiometer circuit	40
Figure 6: A schematic for the excitation circuit of the FlexiForce transducers	41
Figure 7: Breadboard Circuit.....	42
Figure 8: Assembly step 1 for breadboard circuit configuration	43
Figure 9: 5V voltage regulator used to regulate voltage through circuit	44
Figure 10: Assembly step 2 for bread board circuit configuration	45
Figure 11: Side view of assembly step 2 for bread board circuit configuration	46
Figure 12: Assembly step 3 for bread board circuit configuration	47
Figure 13: Assembly step 4 for bread board circuit configuration	48
Figure 14: Assembly step 5 for bread board circuit configuration	49
Figure 15: Assembly step 6 for bread board circuit configuration	50
Figure 16: Assembly step 7 for bread board circuit configuration	51
Figure 17: Assembly step 8 for bread board circuit configuration	52
Figure 18: Assembly step 9 for bread board circuit configuration	53
Figure 19: Assembly step 10 for bread board circuit configuration	54
Figure 20: Final assembly step 11 for bread board circuit configuration, all components wired.	55
Figure 21: Image of a pair of feet and exactly where the force transducers were place on the right heel (indicated by the black dots).....	57
Figure 22: Spinal Rotation Device with Fanny Pack on a Female (to the left) and Male (to the right) Subject; shown from side angle and from behind.....	58
Figure 23: Stationary image of subject with Trackers on the Center of Masses (to the left); Still shot image, tracking of subject while in jogging gait (to the right)	59
Figure 24: Process of Potentiometer Calibration	63
Figure 25: Potentiometer Calibration measured volts from -45 to 45 degrees where 5 degree increments were recorded. (Excluding -5 and 5 degrees).....	65

Figure 26: Calibration Curve of Force Transducer 66

Figure 27: Calibration of Force Transducer using a weight anchored directly on the sensing area of the Force Transducer 66

Figure 28: Visual of recorded data from DAQ box using Pocket Logger XR440 software. 68

Figure 29: The Inverse Pendulum Theory 70

Figure 30: Free body diagram of the foot with muscles 73

Figure 31: Free body diagram of the knee with muscles 74

Figure 32: Plot of spinal rotation vs. pressure for exaggerated spinal rotation test. 77

Figure 33: Plot of spinal rotation vs. pressure for normal spinal rotation test. 77

Figure 34: Plot of spinal rotation vs. pressure for restricted spinal rotation test. 77

Figure 35: Angular velocity of the foot from heel strike to toe off 79

Figure 36: Angular acceleration of the foot from heel strike to toe off 80

Figure 37: Acceleration in the x-direction of the foot from heel strike to toe off 80

Figure 38: Acceleration in the y-direction of the foot from heel strike to toe off 81

Figure 39: Angular velocity of the knee from heel strike to toe off of gait cycle 81

Figure 40: Angular acceleration of the knee from heel strike to toe off of gait cycle 82

Figure 41: Acceleration in the x-direction of the knee from heel strike to toe off of the gait cycle .. 82

Figure 42: Acceleration in the y-direction of the knee from heel strike to toe off of the gait cycle .. 83

Figure 43: A plot of Spinal rotation vs. the angle of the tibia upon heel strike (initial impact). 84

Figure 44: A plot of Spinal Rotation vs. Stride Length 85

Figure 45: Plot of spinal rotation vs. ground reaction force (body weight) for 86

Figure 46: Final Spinal Rotation Design 92

Figure 47: Spinal Rotation Device in Proportion to a Body 92

Figure 48: Shows a 100K-Ohm Linear-Taper Potentiometer 94

Figure 49: *FlexiForce* Force Transducer used for force measurement 95

Table of Tables

Table 1: Weighted Design Matrix	33
Table 2: Calibration of Potentiometer Data	64
Table 3: Preliminary Function vs. Means tree. This helps to understand the preliminary steps to further understand what we chose as our final design.....	90
Table 4: Outline of Materials for the Spinal Rotation Design.....	93
Table 5: Specifications of 100K-Ohm Linear-Taper Potentiometer.....	94
Table 6: Specifications of the FlexiForce force transducer.....	95
Table 7: Heel strike pressure measurements for force transducers 1 and 2	96
Table 8: Spinal rotation measured in degrees for exaggerated, normal, and restricted rotation.	97
Table 9: Compilation of various parameters from video analysis.	98
Table 10: Angular Accelerations of the tibia for the three running forms	102
Table 11: Compilation of the forces experienced in lower leg using musculoskeletal models and computational bioanalysis.....	103

Executive Summary

Locomotion is an essential part of people's daily lives. Studying a person's walking and running form is important because it allows for a better scientific understanding of the different roles each portion of the body has during the gait cycle. With further understanding of a person's form comes the ability to diagnose injury, which can stem from their imperfections. The gait cycle is an important concept, which was developed to describe the cyclic motions that occur in animals while walking or running.

Gait analysis has been researched for many years; early studies, due to lack of technology, relied on means of observation as the only way in which information was gathered. With the progression of technology came the progression of methods of collecting quantitative and qualitative data. The types of devices that helped advance the study of gait analysis include force measurement devices, accelerometers, and video analysis. These devices combined with scientific approach enhanced the knowledge of proper walking motion and form. With the progression of biotechnology, a new level of development and understanding of how the human body functions from a mechanical standpoint has arisen. The gait cycle has many applications in today's society, increasing the need to further expand the knowledge of the walking and running form.

The goal of this project was to study the effects spinal rotation has on the magnitude of the impact forces in the foot and to analyze the ankle and knee joints, to determine what style of running reduces the chance of injury in the joints. The experiment was conducted by attaching foot transducers in the test subjects shoe to record the ground reaction forces and attaching a spinal rotation device their back to record the degree of rotation during the gait cycle. The data was stored remotely on a pocket data logger (also attached to the subject), allowing the experiment to be done on a run way without external wiring, thus freeing the subject and allowing for a more natural gait cycle. A video camera and fixed tracking markers placed on the leg of the subject were used to record the subject so that body segment angles could be found as well as dynamic forces calculated. The data collected was analyzed for the use of calculating the forces in the ankle and knee; the force body diagrams were developed to solve for the unknown muscle and joint force.

The expectation from this experiment was to prove that the forces acting upon the leg would be reduced based on the degree of spinal rotation.

Several preliminary designs were developed for the spinal rotation device and the foot transducers. The foot transducers segment consisted of two force transducers attached to an insole placed inside right shoe of the test subject. The spinal rotation device was comprised of two wooden dowels connected in the middle by a linear taper potentiometer. Both the lower and upper wooden stems had a thin aluminum plate attached that allowed for accurate spinal rotation measurements to be collected. The aluminum plates had Velcro straps fixed to them, which were meant to hold the spinal rotation device in place while the test subject was in motion. The device was placed between the T1 and T12 vertebrae of the subject to allow for accurate readings of spinal rotation during the gait cycle.

No correlation was found in this study stating that spinal rotation is directly related to the forces experienced during gait. Due to variables such as variations in gait, flexion of the knee and ankle joints, center of pressure of the subject, and location of impact of each subject, there was no statistical evidence to support our theory.

1. Introduction

Gait analysis is the study of locomotion (gait cycle) in animals, more specifically human motion. Running as an exercise, competitive sport, form of fun, and a form of locomotion has always been a pivotal part of human motion and transportation. In order to properly perform a gait cycle the joints should be able to undergo sufficient movement and be able to bear the force loads that are implemented on the body while undergoing any form of locomotion. If the joints are not able to withstand the forces, not capable of sufficient movement, and in rare cases there is too much flexibility, the body begins to adjust itself in order to bear the loads, which leads to the joints and muscles working improperly or overworking. These imperfections and/or issues in the gait cycle are referred to as biomechanical abnormalities.

The goal of the project was to determine if there was a correlation between spinal rotation and the impact forces felt on the body during the gait cycle. To properly calculate the correlation between the two the group used a string potentiometer to measure the degree of rotation the spinal makes during the gait process. A piezoelectric transducer was used to measure the reaction forces on the body from the ground during the experiment.

The experiments that were conducted involved 20 male and 20 female subjects, ages ranging from 18 to 25 years of age; some were trained runners and others were people who ran for exercise. The subjects were equipped with transducers, a potentiometer and an accelerometer, which will store the information from the transducers while they jogged. The test subjects were asked to perform several different task movements, for example: they were asked to jog normally, then jog with exaggerated spinal rotation, and jog with restricted spinal rotation. After the subjects perform each task, the data was then stored away and analyzed by the group to provide proof or disprove the correlation between spinal rotation and impact forces during the gait cycle. To understand the data recorded from each subject and then analyze the data, the group used computational biomechanics (further discussed in the paper), which also was applied to determine the impact forces on the ankle joints and knee joints. The hypothesized result

was that as the degree of spinal rotation increased, the impact forces experienced in the feet and lower extremities would decrease proportionally.

The information obtained in this project by the group was helpful to understanding the forces on the body while running. Understanding the forces helped understand the injuries that come with certain conditions or running techniques. Athletes that run for long periods, avid runners, and people who are trying to exercise would find the information presented by the group to be useful. The main information presented at the end of the project was the correlation of force vs. rotation during locomotion.

2. Background

Gait analysis of humans and animals has been investigated for centuries, but it was not until the late 19th, early 20th century that major technological advancements have allowed people to better understand the kinematics of human locomotion. Measurement technology and computerized analysis software and techniques are all used to **analyze the gait cycle** with the ultimate goal of understanding how the body reacts to the forces experienced during gait and highlighting biomechanical abnormalities among a range of other applications. The history of gait analysis, the gait cycle, and instrumentation and measurement techniques are all reviewed in the following sections.

2.1 The History of Gait Analysis

Aristotle is accredited with the first known written reference to the analysis of walking (Baker, 2007). Aristotle published his basic theories of human and animal locomotion in “De Motu Animalium”, in which he conjectured about joint mechanics, the gait cycle, and motion based on his observations (Baker, 2007). None of his propositions were ever tested however. The advent of new technologies and techniques have propelled the field of Gait Analysis over the centuries and have allowed scholars to study and gain more of an anatomical and biomechanical understanding of the gait cycle.

It was not until the time of the Renaissance in Europe that science and mathematics began to develop coherently and the mathematical basis of modern gait analysis started to take form (Baker, 2007). Giovanni Alfonso Borelli, one of Galileo Galilei’s pupils, performed the first experiment in Gait Analysis and from this correctly deduced that there must be mediolateral movement of the head during walking. Borelli also studied the mechanics of muscles and was the first to conclude that forces within the muscles and tendons are significantly greater than the externally applied loads (Baker, 2007).

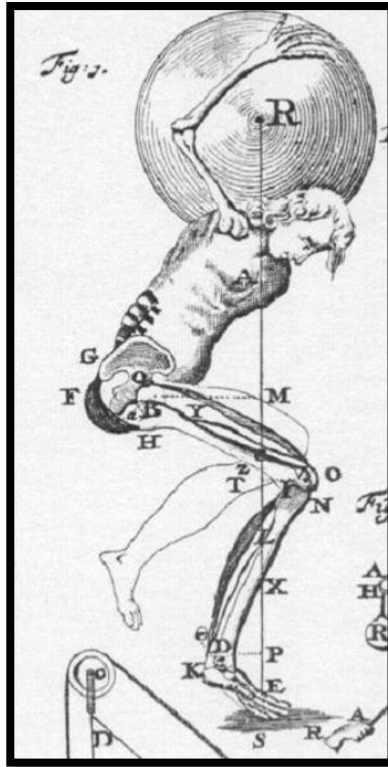


Figure 1: Illustration from Borelli's book on the movement of animals depicting his biomechanical analysis of a man on his toes of one foot bearing a load (Baker, 2007).

After Newton formulated the physical laws governing forces, Hermann Boerhaave was able to utilize them along with Borelli's research to apply Newtonian mechanics to the body and human movement. The brothers Ernst Heinrich and Eduard Friedrich Wilhelm published *Mechanik der Gehwerkzeuge* (Mechanics of the Human Walking Apparatus) in 1836, in which they conducted a considerable amount of experiments using only a stop watch, measuring tape, and a telescope. They were also the first to develop illustrations showing that attitude of the limb segments at 14 different instants in the gait cycle (Baker, 2007).

Jules Etienne Marey worked in collaboration with his student Gaston Carlet to study the gait cycle from a biomechanical and mathematical standpoint, using more sophisticated equipment for measuring impact forces during gait. Carlet developed a shoe with three pressure transducers built into the sole and recorded the forces exerted by the

foot on the floor. He was the first to record the double bump of the ground reaction (Baker, 2007).

Until the invention of photography, the only means of studying gait was by pure observation. Improvements in photography technology made it possible to more accurately analyze the biomechanics of the gait cycle by examining the photographs of precise moments during gait. Marey developed a shutter, which enabled several different images to be captured on the same photographic plate (the chronophotograph). Another one of Marey's students Georges Demeny and Marey himself experimented with the chronophotograph and different types of markers. They recorded several phases of movement onto one photograph with the use of markers; this technique resulted in images from which it is clearly possible to make accurate measurements of the movement and positioning of the limbs throughout the gait cycle (Baker, 2007). By having multiple phases on one photograph it allowed for easier analysis of motion (Braun, 1992).

Willhelm Bruane and Otto Fischer utilized photography as well as their knowledge of mathematics and Newtonian mechanics to conduct the first three dimensional gait analysis (Braun, 1992). They simplified the body to a series of rigid members, which then allowed the forces throughout the body to be studied in three dimensions. Points were measured on the images from each of the cameras on the respective side of the subject, resulting in a full three- dimensional reconstruction of the position of the point calculated (Braun, 1992). Using a full inverse dynamics approach he was thus able to calculate the joint moments for the lower limb joints during the swing phase of gait, laying the framework for three dimensional analysis experiments that would follow.

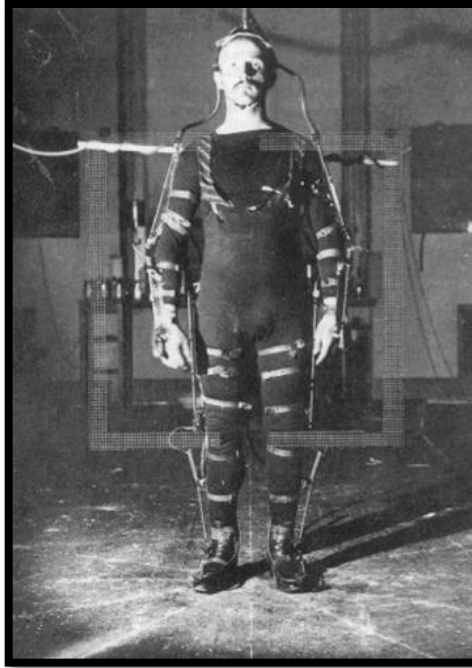


Figure 2: A subject of Braune and Fischer's wearing an experimental suit (Braun, 1992).

It was not until the early 20th century that accurate three component ground reaction forces could be measured. In 1916, Jules Amar was the first to develop a three-component force plate; this had a mechanical mechanism compressing rubber bulbs and pneumatic transmission of the signals similar to Demeny's approach (Baker, 2007). This was a significant contribution to field of gait analysis as three component force analysis could be conducted and applied in combination with photographic biomechanical analysis of gait. Elftman later made a full three-component mechanical force plate at Columbia in 1938 and made the first publication of a study utilizing a force plate. Elftman not only developed the practice of measuring the ground reaction forces but also the pressure distribution under the foot and the theoretical analysis of the forces, moment and energy changes in the leg during walking (Baker, 2007).

Modern gait analysis techniques involve the use of instrumentation such as force transducers, accelerometers, HD camcorders, and force and gait analysis software to name a few. Such advancements in technology have provided a faster, more efficient, and more accurate means of gathering quantitative data for analysis. With force transducers and accelerometers are becoming smaller and smaller and computer software is

becoming more advanced, scientists and scholars are able to conduct more complex experiments for a deeper understanding and further advancement in the biomechanical analysis of the gait cycle.

2.2 The Gait Cycle

2.2.1 Walking

Human gait is the repetitive cyclic pattern of walking or running. This sequence of lower limb motion drives the body forward while maintaining balance and stance stability. The gait cycle is divided into two main phases: the stance phase and the swing phase. While there is a general accepted breakdown of the gait cycle, people display different tendencies throughout their gait; hence no two gait cycles are exactly the same. Factors such as velocity and force distribution alter gait from person to person.

The stance phase constitutes the periods at which a foot is in contact with the ground. About 60% of the gait cycle is comprised of the stance phase when walking and the remaining 40% of the gait cycle equates to the swing phase (Pribut, 2010). During walking, a period called double stance phase begins and ends the stance phase, in which both feet are in contact with the ground. The stance and swing phases can be further split into subdivisions.

There are four subdivisions of the stance phase: the heel strike, foot flat, mid stance, and toe off phases. The heel strike phase represents the period when the heel of an individual's foot contacts the ground. The foot flat phase is the point at which the entire foot is in contact with the floor. The mid stance phase is the period at which weight is transferred from the rear to the front of a person's foot. The three phases above make up the entirety of the double stance phase. Lastly, the toe off phase signifies the pushing off of the toes, creating a propelling motion (Pribut, 2010). Single limb support is initiated during this phase as the foot is lifted from the ground and prepared for swing while the other limb bears the load. (Perry, 1992)

The swing phase is split into three subsections. These sections are known as the acceleration phase, the mid-swing phase, and the deceleration phase. The acceleration

phase is the period from toe off to maximum knee flexion in order for the foot to clear the ground. The mid-swing phase is the period between the maximum knee flexion and the forward swing of the tibia to a vertical position. The deceleration phase is the period between the vertical positioning of the shin to the end of the forward motion before heel strike (Pribut, 2010).

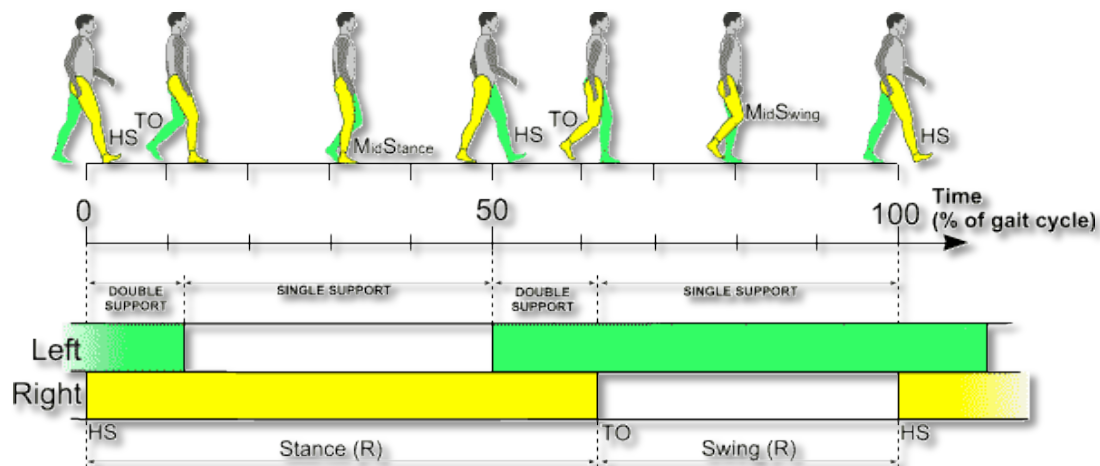


Figure 3: A breakdown of the human gait cycle and how weight is transferred from stance phase to swing phase. HS represents heel strike and TO represents toe off (Pribut, 2010).

Walking faster correspondingly increases the time at which the body is in single stance and shortens the two double stance intervals. When running, the swing phase represents a larger portion of the gait cycle as the foot is in contact with the ground for shorter periods of time. There are also subsequently no double stance phases, and instead there are periods where neither foot is physically in contact with the ground. This is known as the flight phase.

2.2.2 Running

During the running gait cycle, single limb support is the only form of the stance phase but it is comprised of three sub-components: initial contact, midstance, and propulsion (199, Christensen). The ball of the foot makes initial contact with the ground with most of the weight on the outer edge. A gradual shifting of weight to the inner edge follows as the foot moves down and inward to the position of pronation (2010, Pribut). The arch then flattens to distribute the force of the heel strike. Next is midstance, which is the period when weight shifts from the posterior to the forefoot

(199, Christensen). At this point in time body weight is shifted directly over the foot. Pronation ends as the foot begins to roll forward and upward. The final component is propulsion, where the foot effectively becomes a lever with the Achilles tendon providing a pulling force and the ball of the foot serving as a fulcrum (1999, Christensen). The joints in the big toe and forefoot create enough force to launch the foot off the ground and into swing phase.

2.2.3 Alternative Running Styles

There are many relatively new running and walking techniques, which are becoming more prevalent; the objective of some of these styles is to provide a better technique implementing knowledge on how forces are distributed throughout the body while running to reduce the likelihood of common injuries associated with running.

Chi Running, a new running style, was recently developed over the past 35 years by Danny Dreyer, an ultra-marathon runner and student of Tai Chi (ChiLivingInc). The principles of Chi Running are based of the principles taught in yoga and Tai Chi, where the main objective is to maintain balance and return the body to its centerline while running. There have been numerous studies conducted to better understand how forces are distributed throughout the body while running and the causes of common injuries associated with running.

2.3 Injuries

2.3.1 Achilles Tendinitis

The Achilles tendon is the largest tendon in the body. It requires a lot of blood in order to stay healthy and continue working properly. According to Mazzone and Mccue in the article Common Conditions of the Achilles tendon, the Achilles tendon is venerable for injury because of several main reasons. Velocity sports such as running greatly increase the chance of injuring this tendon, as well as an increase in age. This vulnerability is mostly due to the many different forces all acting on the Achilles from many different angles, as well as the limited blood supply compared to the amount of blood it needs. One of the reasons

for the increased frequency of Achilles injuries in the USA as of late is that the ageing population is remaining very active (Mazzone & Mccue, 2002).

As mentioned, Achilles tendonitis is a common injury in the running world. Achilles tendonitis can be found in approximately 10 percent of runners (Mazzone & Mccue, 2002). This is probably due to the fact that while running there are forces on the Achilles up to eight times body weight. Not only is this a lot of stress, but it persists for long periods of time. It takes a long time for the body to become use to these kinds of stresses. This is why Achilles tendonitis occurs most often in new athletes (Mazzone & Mccue, 2002). Even normal gates have lots of motion on the Achilles, leading to increased chance of injuries. However, there are many runners who have incorrect technique. This, along with the fact that many new and even some experienced runners, wear shoes that do not fit properly, are a significant factor in the onset of Achilles tendonitis. Specifically hyper-pronation, a condition common in new runners, as well as contracture of the gastrocnemius-soleus complex are tendencies that lead to this injury (Mazzone & Mccue, 2002).

Achilles tendonitis is not an injury that runners can get over quickly. Symptoms tend to last for several months. Mazzon and Mccue fount that “One study showed that 56 percent of competitive track and field athletes with Achilles tendonitis discontinued all sporting activities for a minimum of four weeks to promote healing” (Mazzone & Mccue, 2002). The drawn out recovery time is due to the nature of the injury. “Tendinitis is a diffuse thickening of the tendon without histologic evidence of inflammation caused by intertendinous degeneration’ (Mazzone & Mccue, 2002). It takes time for the increased size of the tendon to come back down. Typical treatment for this type of injury is rest, ice, anti-inflammatory medicine and physical therapy.

2.3.2 Shin Splints

One of the most common distance runner injuries are shin splints. “In a study by Reinking (2006), 50% of collegiate cross country runners (nine of 18) experienced shin splints over the course of a competitive season, while 94% of them had suffered at some point in their running career” (Newlin, 2011). Shin splints are when an athlete experiences

pain in the front region of the lower leg, specifically the Tibia, the tendons connected to the Tibia and the other soft tissue surrounding the Tibia.

The cause of shin splints is when there is damage to the tibia from repeated stress. This damage consists of small fractures and lesions to the Tibia. As shin splints worsen into the chronic level, uneven edges can be detected even without any medical instrumentation. These uneven surfaces indicate “that bone was being broken down and reformed there as a result of repeated stress” (Newlin, 2011). Where the bone had been broken down, there are new bone growths; this could be the main source of the pain (Newlin, 2011).

There are several theories behind what causes the bone to break down in the Tibia; however the most popular cause is due to over pronation. This is due to the fact that shin splints are found more in runners that pronate compared to those who do not. “Bennett, Reinking, Pluemer, Pentel, Seaton and Kilian (2001) studied causes of shin splints in high school runners and found a significant relationship between over-pronation and shin splints. Runners with greater than normal drop measurements were more likely to develop shin splints” (Newlin, 2011). Pluemer, Pentel, Seaton and Kilian are not the only ones to find a correlation between pronators and shin splints. “In a study by Michael and Holder (1985), seven out of eight runners with shin splints had over pronated feet” (Newlin, 2011). Besides over pronation there are other factors that increase the risk of shin splints. Spending too much time running on paved roads, hills, uneven surfaces, and running indoors are all factors that increase the chances of shin splints. All of these factors, including over pronation, result in the arch collapsing when it is bearing the load of the body. This repetitive forces being exerted on the foot are the direct cause of shin splints (Newlin, 2011).

2.3.3 Runners Foot Injuries

Besides the Shins, and the Achilles there are many other injuries that runners experience all in the foot area. Most of these injuries are due to perpetual impact on the foot before it is properly conditioned to deal with these repetitive stresses. According to Waiden, cited in the article *Common Runners/Walkers Foot Injuries* written by McDaniel,

Ihlers, Haar, Jackson and Gaudet, runners have 37-56% risks of injury during a year's time of training (McDaniel, Ihlers, Haar, Jackson, & Gaudet, 2010).

Plantar fasciitis is once such common injury among runners. "Plantar fasciitis develops as a result of tension mat occurs in the plantar fascia during extension of the toes and depression of the longitudinal arch during weight bearing activities" (McDaniel, Ihlers, Haar, Jackson, & Gaudet, 2010). According to Rachelle Buchbinder plantar fasciitis is the result of 10% of all running injuries (McDaniel, Ihlers, Haar, Jackson, & Gaudet, 2010).

Ankle instability is a problem that leads to many other injuries. Runners with a history of ankle sprains are predisposed to acquiring more ankle sprains in the future (Drewes, McKeon, Kerrigan, & Hertel, 2009).

Another injury found in runner is injuries of the mid-foot. Although this injury is relatively rare compared to the other common running injuries, when it is present, it is often misdiagnosed as a sprain. The ridges structure of the mid foot is a contributing factor to causing this injury (Makwana & Liefland, 2005).

Stress fractures are also a common injury found in runners. Its causes are similar to that of many other running injuries including changing in training surfaces, improper foot were, changes in training, specifically hills, prolonged running on hard surfaces and a sudden increase in mileage. Stress fractures can sometimes occur when injuries, such as shin splints, go unattended for a prolonged period of time (McDaniel, Ihlers, Haar, Jackson, & Gaudet, 2010). They are structural deformities in the surface of the bone. According to DcDaniel, Ihers, Haar, Jackson and Gaudet, the "most common type of metatarsal stress fracture involves an injury to the stem of the second metatarsal" (McDaniel, Ihlers, Haar, Jackson, & Gaudet, 2010).

3. Instrumentation and Devices

When studying the gait as well as spinal rotation there are different instruments and devices that are technologically advanced enough to analyze data captured. The methods that are used to measure the gait cycle and spinal rotation include accelerometers, potentiometers, and goniometers. These methods are discussed further on the following pages.

3.1 Accelerometers

An accelerometer can measure the vibration or change in motion of a structure. Forces caused by the change in motion causes the mass studied to distort the piezoelectric material which can distribute an electric charge that is proportional to the force exerted upon it (2003, OMEGA ENG). The charge measured is proportional to the force and because the mass is constant, then the charge can be interpreted as the acceleration. The acceleration has a direction and a magnitude. It is measured in terms of gravity or $9.81 \text{ (m/s}^2\text{)}$ (2003, OMEGA ENG).

One type of accelerometer is called Piezoelectric. Piezoelectric transducers are used to measure shock sensing devices. There are piezoelectric crystals, those that are made of quartz or ceramic that distributes an electric charge when a force is exerted by a mass under some change in motion. Quartz plates, made of two or more, are preloaded so that a negative or positive change in the applied force on the crystals result in a change in the electric charge (2000, Eibeck). The Piezoelectric accelerometer has the highest range, measuring up to 100,000 g's but unfortunately has low sensitivity compared that to other accelerometers.

Another type of accelerometer is called the vibrating element; it can measure vibrations by acquiring the displacement of a seismic mass that varies the tension of a tungsten wire in a permanent magnetic field. The wire will vibrate at a particular frequency when an electric current is resonated. The circuitry will then output a deviated frequency from that of the centered frequency and because this is proportional to the applied acceleration precise data can be recorded (2000, Eibeck). A couple of drawbacks in using

this accelerometer are that it is quite expensive and extremely sensitive to temperature variation.

3.2 Potentiometer

A potentiometer also known as a “voltage divider,” is made of three-terminal resistors with a sliding contact. This device is used to control electrical devices such that of audio equipment but more importantly this MQP will be using the potentiometer to measure displacement transducers. This device usually weighs no more than 5 pounds and can measure a voltage no more than an amp (2011,WIKI).

The potentiometer would be a significant device used in this project because the sliding contact in the device moves across the resistive element, the resistance will change and since the rotation accounts for the angle change the voltage of the potentiometer will output proportionally. This will allow the team to be able to accurately measure the spinal rotation in degrees once converted from voltage.

The potentiometer the MQP will be using is one that measures rotation. There are potentiometers that are capable of moving in 6 degrees of freedom, but in our case we will want a simple linear taper potentiometer that involves a holder across the back of the subject or a string potentiometer. The positioning of the device will infer how the subject moves their spine and by analyzing this rotation the team will see a correlation between this and the gait using accelerometers.

3.3 Video Analysis

To account for the range of motion of the upper body a potentiometer was used as a viable device as well as used in unison with video analysis with 2-D modeling it then took still shots to help understand the measure of rotation over time. The group analyzed the different angles of our subjects initial, during and ending gait that helped the MQP team fully understand how the range of motion changes in time. Goniometry is another term to define video analysis as well as incorporating the visual component of cameras; The MQP team will be using these two main types throughout the project.

The different devices the Academic Technology Center (ATC) provided impact on our quality of the video analysis. One device is in the form of a camcorder. The device is called "Sony HDR-XR500V Hard drive Camcorder," This camera has a built in hard drive so there is no need for a memory stick, its resolution is of High Definition with a LCD touch screen panel (2009,ATC). The team believed that by using this camera we would not only be able to record our subjects running but also take still shots that will dramatically help our analysis of the gait.

Another device the MQP team used to take still photos is called the "EX-ZR100" camera. This camera involves a memory card that the MQP team was aware of to make sure that we could record our subjects accurately. The resolution incorporated a 10 mega pixel display lens with a file size of 517KB as well as measuring the video at a rate of 240frames per second (2009,ATC).

4. Project Strategy

Sixty-five percent of runners experience an injury in an average year (Incidence and Injury, 1993). New alternative running methods, such as Chi Running, states that with more spinal twist, the tendons and ligaments act as a rubber band to propel the body back to its natural position (Dryer, 59). The alternative running methods currently do not have numbers supporting the theory, but it is clear that there is a need for a way to reduce the injuries that occur in runners.

4.1 Problem Statement

Spinal rotation in the gait cycle and its relation to impact forces in the foot is a field lacking quantitative data that provides proof/disproof of the theory. This experiment studied the hypothesis that increased spinal rotation during the gait cycle reduces the forces experienced on the body. The study conducted aimed to measure the forces on the knee and ankle and the amount of spinal rotation during a normal, exaggerated and restricted jogging gait cycle. Computational biomechanics was studied to identify the resulting forces found in the ankle and knee. In order to study this hypothesis, a spinal rotation device and a scientific method of measuring the forces experienced upon landing were needed.

4.2 Objectives

The major objectives the team focused on were safety, manufacturable, repeatable, comfortable and durable.

- In respect to safety, if the device failed it must not harm the user, for example it must not send out an electric current into the user or a piece of the device must not protrude into the user.
- The device needed to be manufacturable, meaning the device needed to be easy to build and also needed to be built at a reasonable cost (>\$600).
- The device needed to be repeatable meaning users can use it universally and it is also needed to be versatile but the data that is outputted had to be precise and accurate. Universally the device is accommodating, easy to assemble, and able to

be used on different terrains (i.e. flat and uneven surfaces). The device should be an insert, which can universally fit into most, if not all types of running shoes.

- Comfortability of the user is also an objective, the device should not restrict the gait cycle of the user. Simply meaning the device should be unobtrusive and lightweight enabling the user to use the device without any change in their normal tendencies.
- Durability of the device is also essential; it must measure up to 1000 Newtons of force without fail and accurately measure the data.

4.3 Constraints

The major constraints the team focused on were:

- The device needed to be able to be setup in no more than 5 minutes. The time it takes to setup the device should not become bothersome to the user.
- It needed to accommodate users between 150 lbs – 190lbs. With this range of weight class, more users can use the device without fail.
- It also needed to accommodate the height range of 5 ft to 6 ft. With this range in height, the device can be used by more without having trouble accommodating for the people below or above average height.
- The device needed to not be obtrusive to the runner. The gait cycle of the user was what was being analyzed so the device cannot inhibit the user's gait cycle.
- It needed to also last up to 7 weeks before failing. The data recording process took approximately 7 weeks so the device could not have failed mid data recording time, so it needed to last past the given 7 weeks.
- The device also must not hurt the user in any form, for example it must not cause blisters on the user. While the user is working with the device, the device must not harm the user causing minor cuts, minor bruising, or any form of harm to the user.

Without these constraints being met the project would not have successfully be completed.

4.4 Functions/Specifications

The function of the final design was the absolute key to envisioning how the group would utilize it in the best way possible. According to Appendix A the preliminary functions and means were to help the group understand what materials would be best fit for the spinal rotation device on the upper torso and the force transducer device on the feet. The specifications would help the group understand what exactly is being attached to the user.

In the final design the spinal rotation device had to measure rotation of the spine around the y-axis in mid gait and the way the group accurately represented this was by using an 100K-Ohm Linear-Taper Potentiometer(refer to Appendix D), measuring the resistance of each rotation with an emphasis on the degree of that rotation. The group acquired data from spinal rotation and recorded the voltage outputs onto a portable storage device by using a data acquisition box. The next function was the attachment to the back of the user and how the group would provide adjustability; the group satisfied this function by using Velcro straps across the chest cavity and over each shoulder of the user attached to the aluminum metal alloy of the spinal rotation device. The breadboard inferred the collection of the voltage of the potentiometer and the impact forces on the feet to the data acquisition box; it was powered by a 9-V battery.

The group decided to monitor the movement of the user by using 2-Dimensional still shots acquired from the Academic Technology Center (refer to Appendix F). This helped the group see the displacement of each user in mid stride. The group then correlated the data collected to see if the displacement of the user mid gait had any effects on the speed of the user in any way.

The functions of the final design for the lower body were important to distinguish as well. One main function was the measurement of reaction forces on foot during gait cycle and the group decided to use two “Tekscan *FlexiForce*” transducers to measure these impact forces. The group acquired data using the same data acquisition box used for the spinal rotation device. Using 28 gauge wires the data from the spinal rotation device and force transducers were transmitted to the daq box.

5. Alternative Designs

There were two components that required a design aspect for the study: the foot transducers and the spinal rotation device. Each component had to be designed separately but with the idea of integrating each into a single data logger with four input channels, one of which would be used as an on/off switch. Before the final design of the foot transducers and spinal rotation device, preliminary concepts and designs were first developed. The alternative designs were developed and the best design was chosen to test for initial results.

5.1 Foot Transducer Component

Since the group decided upon using force transducers as the method of measuring force, each design was based off the idea of having force transducers placed into one of the insoles of the shoes.

5.1.1 Design 1

Design 1 shows two force transducers, one located in the forefoot and one in the heel, in order to measure force during heel strike and toe off while in gait. The transducers were placed on the center of pressure locations as determined by literature and using a force plate. However this design was limited as there was only one transducer in each region of the insole, so not all of the forces would be measured as these transducers have a sensing area of 0.375 inches.

5.1.2 Design 2

Design 2 shows three force transducers, similar to design one with one in the forefoot and one in the heel. One additional force transducer is added along the arch of the foot to record force during mid-range of gait cycle. The design was advantageous, as the transducer in the arch would allow the tracing of the center of pressure over the duration of the gait cycle. However this option also had the same limitation as design 1 in the sense that the individual transducers spread out across the insole could not measure all of the force accurately.

5.1.3 Design 3

Design 3 shows three force transducers, all located on the heel of the insole. The configuration allows the analysis of forces during heel strike. The advantage of this design was that it reduced and isolated the area in which the group is examining, so more data could be collected on a specific region. This would provide the most accurate data of the three designs considered. The disadvantage to this option was that no data would be recorded or analyzed outside of the heel region.

5.2 Spinal Rotation Component

The spinal rotation design was split into two parts: a rotation measurement device and a back brace fixation device.

5.2.1 Design 1

In design 1 the spinal rotation design was comprised of a plastic plate with holes, which would allow it to be attached to the main back brace at an adjustable level. Attached to the plastic plate is a potentiometer connected to a voltage source and portable data acquisition and storage device. The potentiometer's rotating stem is connected to a long thin strip of plastic that extends to the midpoint of each shoulder blade (this piece is also adjustable). The rotation in the potentiometer is caused by spinal rotation, which matches to the rotation generated by the spine (refer to Appendix A).

The back brace fixation design is made of three components, two Velcro adjustable straps that allow proper positioning of the device and the plastic fixation plate. The two Velcro adjustable straps are needed so that the plastic fixation plate will firmly rest on the test subjects back without moving. These straps would fit around the torso of the subject. The plastic plate has holes positioned throughout it, allowing for adjustable attachment of the spinal rotation component.

5.2.2 Design 2

Design 2 is not adjustable. The potentiometer's rotating stem is still connected to a voltage source and portable data acquisition box; however no plastic brace is implemented in this design. The wooden dowels would be fixated to the top and bottom of the

potentiometer and the aluminum plates are attached to the dowels using u brackets and screws. The Velcro straps wrap around the shoulders and torso for proper fixation of the device and to ensure that the device did not fall down the back of the subject during testing.

A weighted design matrix was used to determine which design alternative best met our objectives (refer to the table below). The weighted design matrix allowed the group to assign an amount of importance to each objective and then rate each alternative design on a scale of 1 to 3 on how well it met the objective. The total for each design alternative was the average of the accumulated ratings.

Table 1: Weighted Design Matrix

Objectives	Weight	Spinal Rotation Device		Force Transducers		
		Design #1	Design #2	Design #1	Design #2	Design #3
Safe	0.3	3	3	3	3	3
Manufacturable	0.15	2	1	2	2	3
Repeatable	0.25	3	1	2	1	2
Comfortable	0.1	2	2	1	1	2
Durable	0.2	3	1	2	2	3
Total:	1	2.75	1.7	2.2	1.95	2.65

Rating system:

Each category was assigned a weight based on the overall importance to the design. The weights of all the objectives add up to 1. Each design was assigned a rating of 1-3 for how that design was selected in best possible outcome.

3-Superior Performance

2-Fair Performance

1-Poor Performance

Each category ratings were multiplied by the category weight and added together for each individual design.

The total row shows each of the design's performance.

6. Final Design

The final design is broken down into three major parts, the force transducer system, the circuitry/data recording system, and the spinal rotation system.

6.1 The Force Transducer System

The force transducer system consisted of two Tekscan *FlexiForce* A201 transducers, a Dr. Scholl's foot insert, and 28 gauge wires. For more specifications on the Tekscan *FlexiForce* A201 transducer reference Appendix D.

The force transducers were attached to the heel of the Dr. Scholl's insert using an epoxy for a sturdy connection between the two materials. The leads on the ends of the two *FlexiForce* transducers were then fastened to wiring, which added to the security of the connection. The wiring then led up the leg of the test subject and connected to the circuitry/data recording system.

Since only two force transducers could be used, they had to be placed very strategically. It was concluded that the data collected would be most useful if the transducers were placed on the heel, isolating the location in which force impact is being analyzed as explained in the design 3 section above. The subjects were only required to jog, further reducing the number of variables, such as toe striking during data analysis.

6.2 Spinal Rotation System

Design 2 of the spinal rotation component was used to minimize the amount of materials strapped to the subjects back. The group determined that the back brace would affect the gait of the subjects during testing; therefore it was omitted from the final design. Refer to Appendix B for a picture of the final design prototype.

The spinal rotation system was composed of two four-inch by one-inch wooden dowels identical in all dimensions, the top dowel has a 1.25 inch by 0.24 inch hole in the center, an 100K Ω potentiometer, two aluminum back pieces, Velcro straps, metal brackets, a cap for the potentiometer made of plastic, screws and nuts. Four-inch wooden dowels were used because they were not too big or too small to fit on the back of the user and the wood is lightweight but sturdy, allowing it to withstand damage. Aluminum back pieces

were also used because they are not only lightweight but also sturdy, allowing enough bend to fit comfortably around the users back. For more specifications on the materials used for the spinal rotation system reference Appendices B and C.

The wooden dowel were fixed to the middle of the aluminum back pieces using a bracket and two screws and two nuts to fasten the bracket and the dowels to the back of the aluminum pieces. After fixing each dowel to an aluminum back piece the Velcro straps were then attached to the back pieces by epoxy so the users could attach the device to their backs and not have to hold up the equipment while running. The potentiometer's negative, positive, and ground terminals were soldered to three separate wires. A plastic protective cap with a hole at the top covered the potentiometer, protecting the potentiometer's electrical connections but simultaneously allowing the stem of the potentiometer to have unrestricted movement. The cap was then fastened to the bottom dowel using a bolt and a nut. This method allows the soldered wiring and potentiometer to be protected and also allows the group to change the potentiometer in case it breaks or needs to be changed.

After fastening the cap and potentiometer to the bottom dowel, the stem of the potentiometer was placed into the 1.25 inch hole in the bottom end of the top wooden dowel and friction held the stem of the potentiometer in place while allowing the stem to twist and collect data while the user ran and experienced spinal rotation or a lack of spinal rotation. The final step for finishing the spinal rotation system was to take the three wire endings, which were attached to the potentiometer and place them in the designated areas in the circuit/data recording system (further detailed in the next section).

6.3 Alterations to the Final Design

There were a few alterations made to the final design while the group was building the device, which are detailed in the following section.

6.3.1 Dowel Length

In the original designs each dowel length was set to 3 inches. However as the prototype was being made the group looked at the relative sizes and decided that longer

dowels would have a longer lever. This would increase the ability to collect more accurate data. The longer moment arms of the dowels to the potentiometer allowed for easier ability to record the degree of rotation. Also having the metal plates further apart on the test subjects back isolated the plates, which also allowed for more accurate degree of rotation measurements. While it was important to separate the metal plates, the group found that if the plates were too far apart then it would no longer be as versatile because it would no longer be able to fit on smaller test subjects. The length of the two dowels was increased to 5 inches each, which will fit the average subject rather well.

6.3.2 Number of Force Transducers

Ideally the group would have placed force transducers throughout the surface area of the bottom of the foot but there were limitations. The Data Acquisition Box (DAQ Box) only had 4 input connections; one for the potentiometer, leaving only three available inputs. However after further testing with the force transducers and the DAQ Box, a couple more limitations were discovered. The DAQ Box could only record a fairly limited amount of data at a set time interval and the only way to control the interval of recording was to create an on/off switch. Due to these limitations, a clicker was implemented to control the collection of the data, after adding this attachment, there were only two inputs left, meaning the group could only attach two force transducers.

6.3.3 Placement of Force Transducers

Due to the fact that only two force transducers could be used, they had to be placed very strategically. Originally it was determined that the transducers should be spread out over the foot in order to have the most likelihood of getting some substantial data in at least one of the transducers. Later it was concluded that each individual transducer provides a limited insight into the impact forces. Also the group planned on having the subjects jog, with the subjects jogging most subjects would be landing on their heels (heel strike). The group therefore moved the two transducers to the heel. Since most runners tend to pronate, the two transducers were angled next to each other, the back transducer was placed in the center of the very back of the heel and the front transducer was placed on the outside edge of the front of the heel.

6.3.4 On/Off Switch

After testing of the device began, it was quickly realized that data recording started right after the program was downloaded and would continue until there was no space left on the DAQ Box. There was no way to stop and start the recording besides physically unplugging the device. The amount of data storage on the DAQ Box was limited to a small amount, making it very difficult to record long enough to allow the subject to run the tests without rushing and generating bad data. This problem was solved by installing an on/off switch using a push button switch. Due to the dated technology, the button worked a bit unconventionally, when the program was downloaded the button had to be held down; this stopped the DAQ Box from recording data. Respectively once the button was released the DAQ Box would start recording data, when the test was over the button would be clicked to stop recording. In order to start the recording process again the data had to be downloaded to the computer, and the program had to be downloaded again on the DAQ Box.

6.3.5 Connection of Potentiometer to the Dowels

Originally a main focus was to be able to make the dowels interchangeable due to the fact that the potentiometers had been known to fail more easily than any other part in the device. It was then discovered that there would be a problem both fastening the potentiometer and making it easily interchangeable. After a reevaluation period it was determined that since it was the potentiometer that would most likely fail, it would be more productive and make testing much more manageable if the potentiometer was epoxied to the base of the dowel. And if there were an issue, such as the potentiometer malfunctioned, the entire dowel would be replaced. Also it was important that the stem of the potentiometer be able to be pulled out the top dowel whenever required. A press fit hole was drilled into the top dowel so the stem of the potentiometer fit tightly into the top dowel and was held in by friction.

6.3.6 Cover to Potentiometer

Since safety is the number one priority to this project, a cover for the potentiometer is required. The constraints, which needed to be satisfied by this

alternative, are that it must cover the potentiometer, leads included, from accidental touching at any time. However the potentiometer had to also be easily accessible in case any of the leads broke off or any other emergency. The final decision was to use a PVC pipe cap that had a hole drilled into the top to allowing the potentiometer's stem to pass through with plenty of clearance. A hole was also drilled into the side of the cap that went through the cap and the stem. A screw and bolt was inserted through this hole to keep the cap tightly in place, but easily removable at the same time.

6.3.7 Back Plates

The material to be used for the back plates needed to be both pliable and firm. It needed to be pliable because it needed to be bent to conform to the back of each individual test subject but firm because all rotation had be properly recorded, so it could not bend or deform at all under stress applied from rotation. Aluminum was the chosen material for the back plates. Once chosen the next challenge was to figure out how to secure the metal back plates onto the test subject. For the top back plate horizontal slits were made so Velcro straps would go over the shoulders and loop into another fastener that goes around the subject's waist. For the lower back plate, the slits were placed on outermost edge of the back.

6.3.8 Velcro Fastenings

In order to make sure that the potentiometer generated accurate readings it had to be fastened to the body but it had to stay in a fixed point, Velcro straps were used to fill this requirement. The Velcro strips had to be strapped together in order to be strapped to the test subjects back. The bottom metal plate had two different Velcro straps on either side facing in opposite directions; the slack was rolled up on the back so that the two Velcro straps were not too long. The top two strips went over the top of the shoulders to keep the metal plate fastened securely to the back.

6.3.9 Data Acquisition Box Protection

One of the main focuses of the group was to clean up the wired connection and keep the equipment and subject safe. To achieve this goal the group used a fanny pack,

which held the DAQ Box and breadboard but also used the waist fastener of the fanny pack to hold down the Velcro shoulder straps as previously described in the last section. The breadboard and DAQ Box were attached inside the fanny pack in such a manner that the plug-in areas are closest to the zipper of the fanny pack when closed; ensuring the accessibility of the wiring in case of any problems.

6.3.10 Assembly

The assembly process of the spinal rotation device went as follows; first the dowels were fastened to the metal plates, which were done by bolting the dowel to the pipe with a C bracket. The bolts were on the outside of the device, the same side as the dowel, to ensure the safety of the subjects. It was critical that the dowel with the hole for the potentiometer was put on the top plate with the horizontal holes for the Velcro; respectively the plate with the vertical holes was on the bottom. The potentiometer was then centered top of the bottom dowel and covered by the PCP pipe cover with the stem of the potentiometer sticking through the top. The leads to the potentiometer had already been soldered and emerging from under the PCP pipe. Lastly for the spinal rotation aspect of the device, the stem of the potentiometer was inserted into the hole on the top dowel and the leads from the potentiometer were plugged into bread board.

The force transducers were then tapped to a heel insert, which was cut from the full shoe insert. They were placed in the exact manner described above in the placement of force transducer section. The leads of the force transducers were fastened to 28-gauge wiring and plugged into the breadboard.

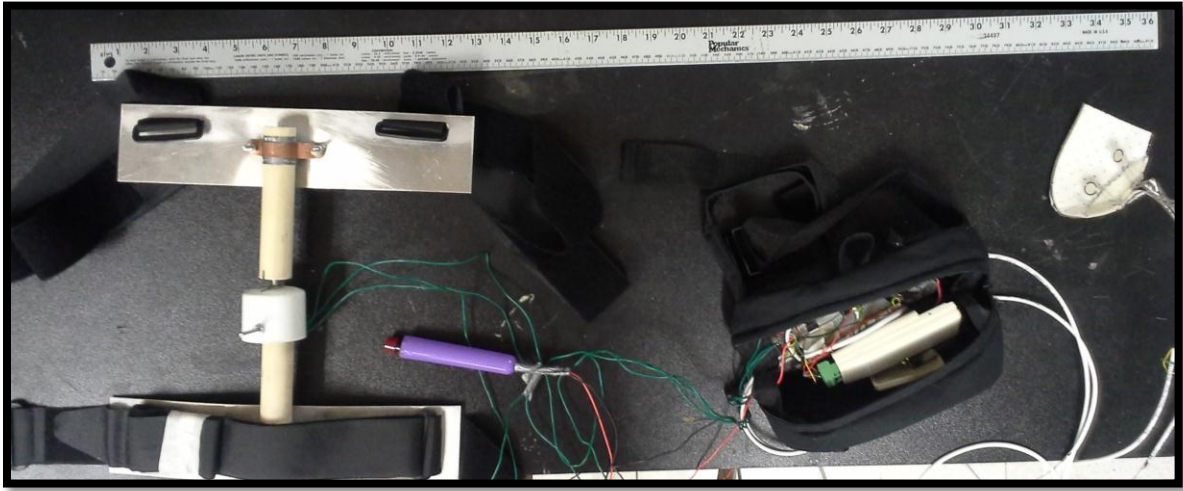


Figure 4: Spinal Rotation Device with Fanny Pack and Force Transducers on Insole.

6.4 The Circuitry/Data Recording System

The breadboard was separated into two sections. The top section was configured for the potentiometer and the bottom section was configured for the force transducers. The MCP6004 I/P quad general purpose op amp was used to enhance the signals from the force transducers and the potentiometer.

The potentiometer has 3 leads. The left terminal was wired in series to the voltage regulator, and the right terminal wired V_{out} to the data acquisition box. The middle terminal was connected to ground. A schematic for the potentiometer circuit can be viewed below in Figure 5.

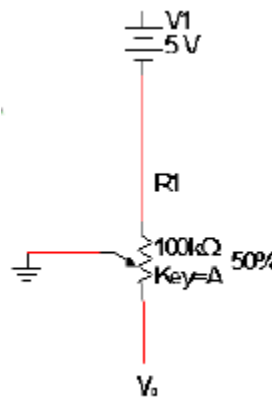


Figure 5: A schematic for the potentiometer circuit

The breadboard was powered by a 9-V battery and a 5-V voltage divider was used to reduce the voltage entering the op amps. The *FlexiForce* transducers act as force sensing resistors in the electrical circuit. The resistance is very high when the *FlexiForce* transducers are not loaded. When a force is applied to the transducer however, this resistance decreases proportionally. Each transducer was connected to an individual op amp. A schematic for the excitation circuit of the *FlexiForce* transducers can be viewed below in Figure 6.

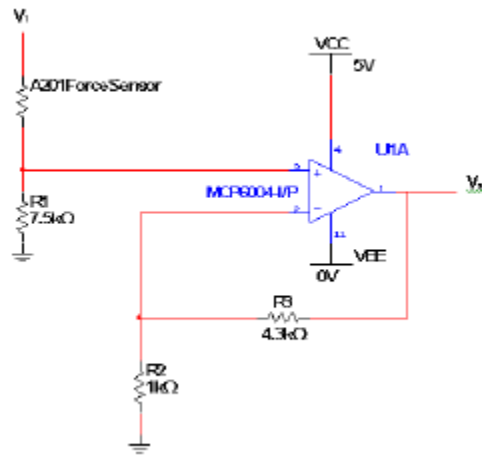


Figure 6: A schematic for the excitation circuit of the FlexiForce transducers

The V_{out} was wired to a Pace Scientific XR440 Data Logger to allow for analysis of the data collected.

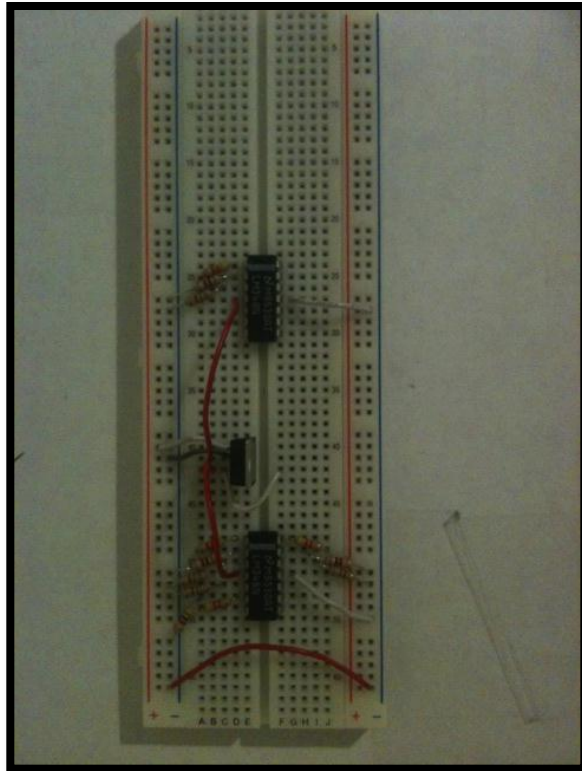


Figure 7: Breadboard Circuit

6.4.1 Assembly

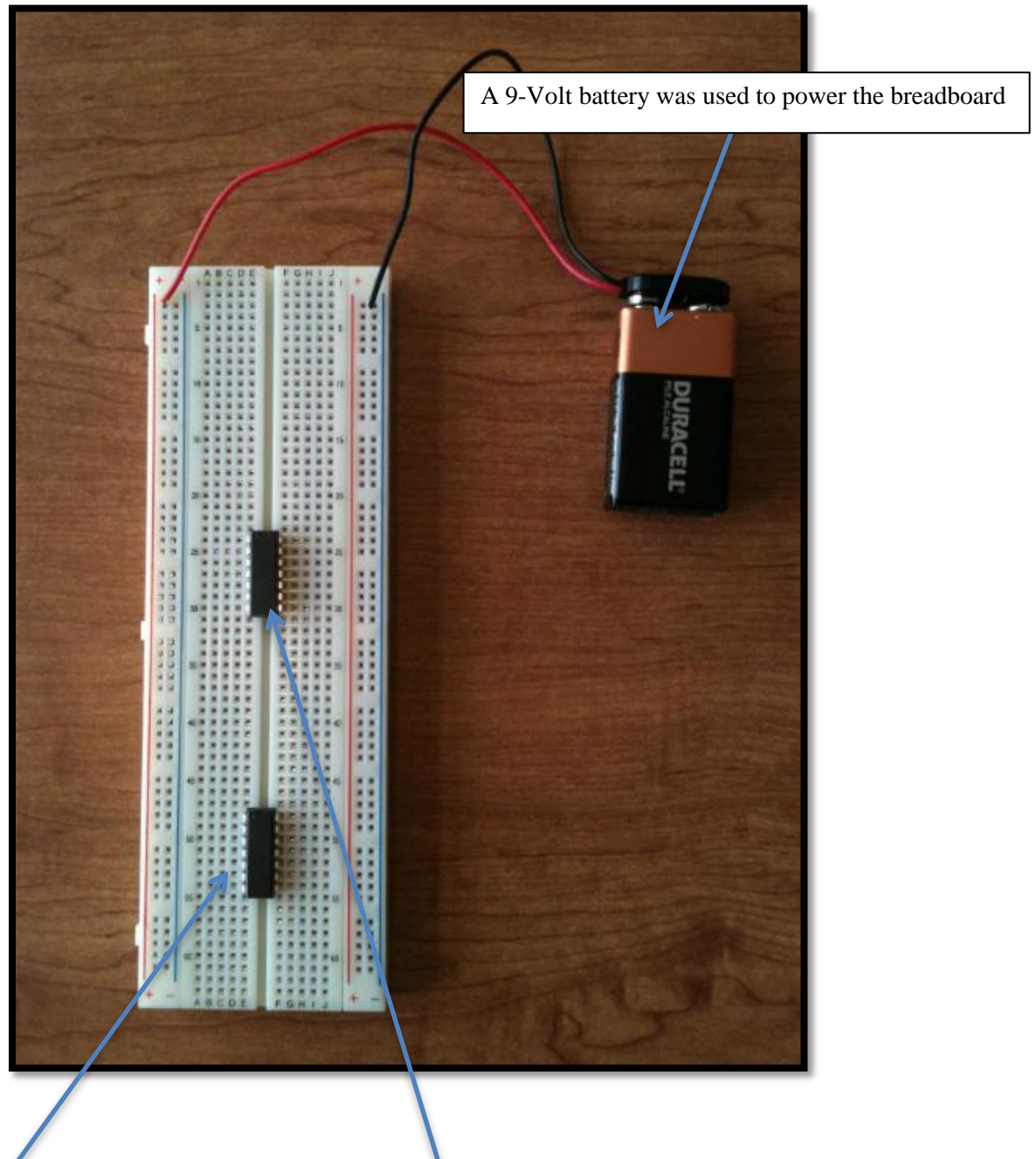


Figure 8: Assembly step 1 for breadboard circuit configuration

A 5-V voltage regulator was used to regulate the 9-V battery. This unit can be found in the Intro to ECE kit.

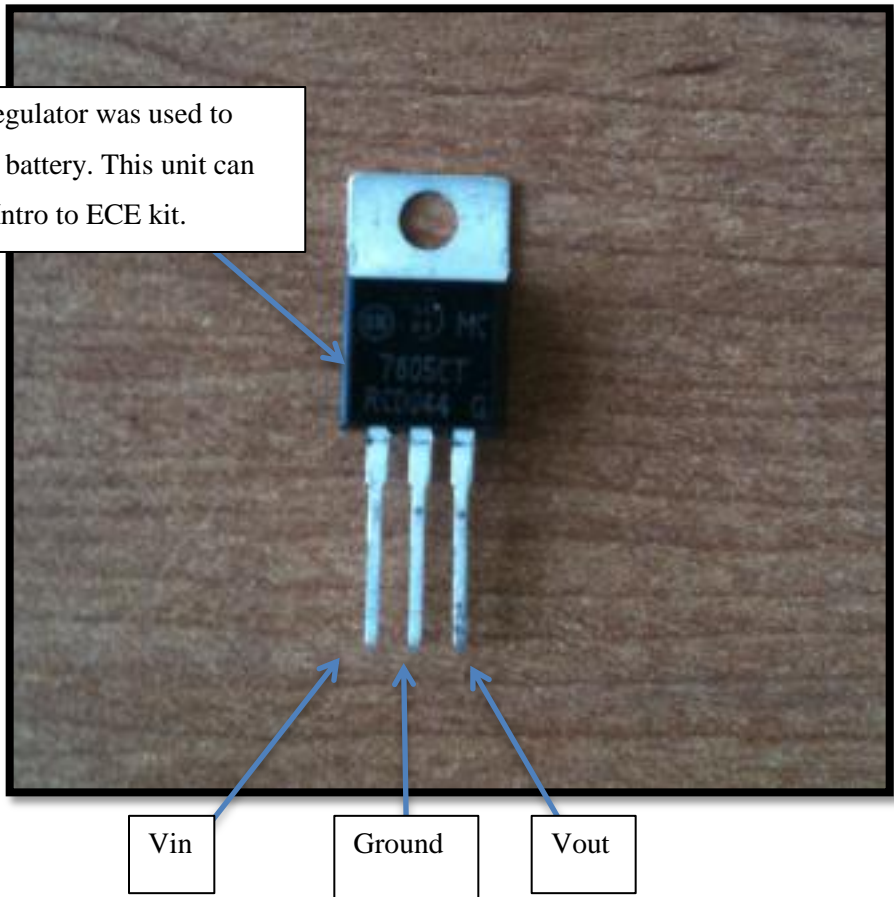


Figure 9: 5V voltage regulator used to regulate voltage through circuit

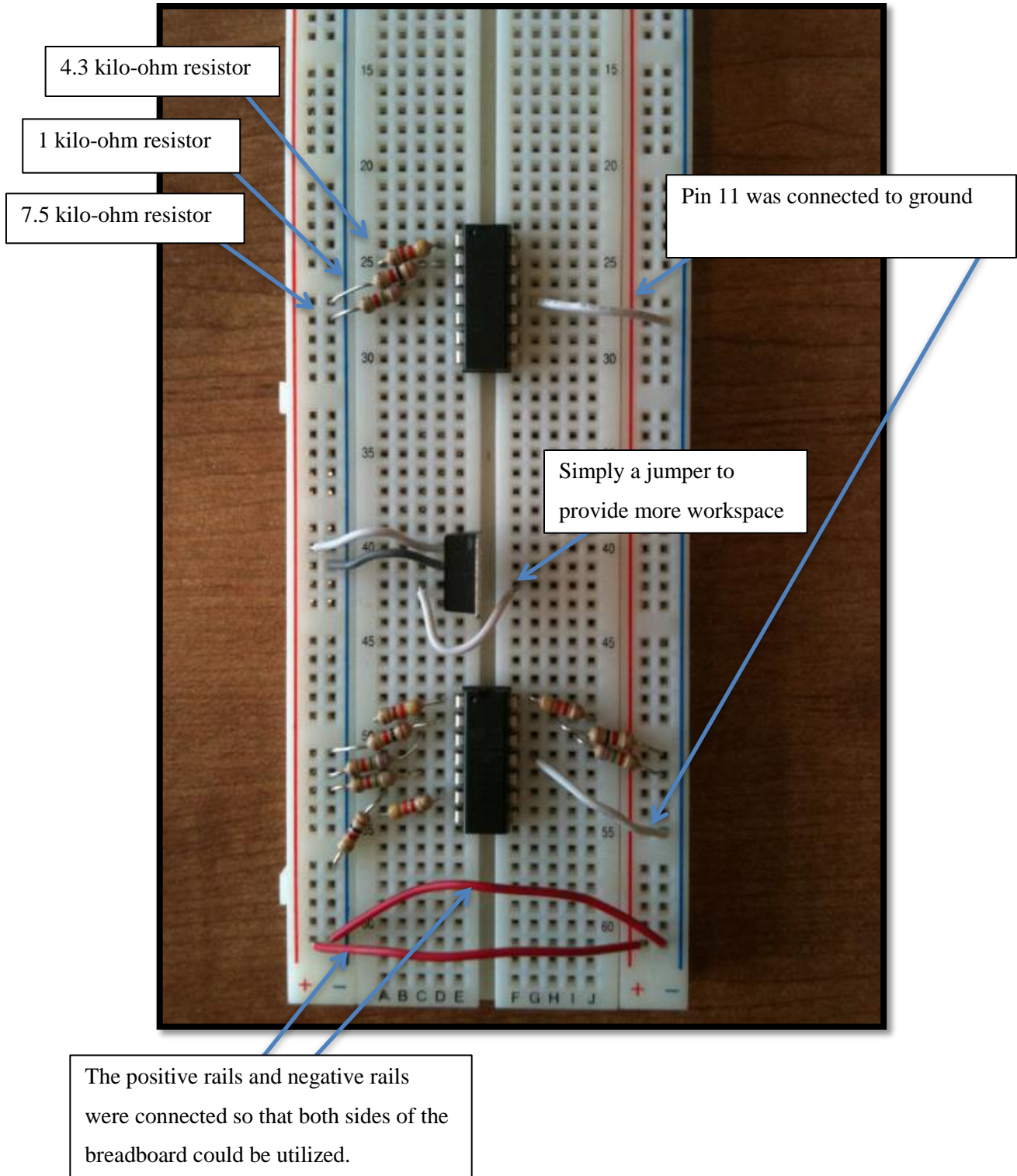


Figure 10: Assembly step 2 for bread board circuit configuration

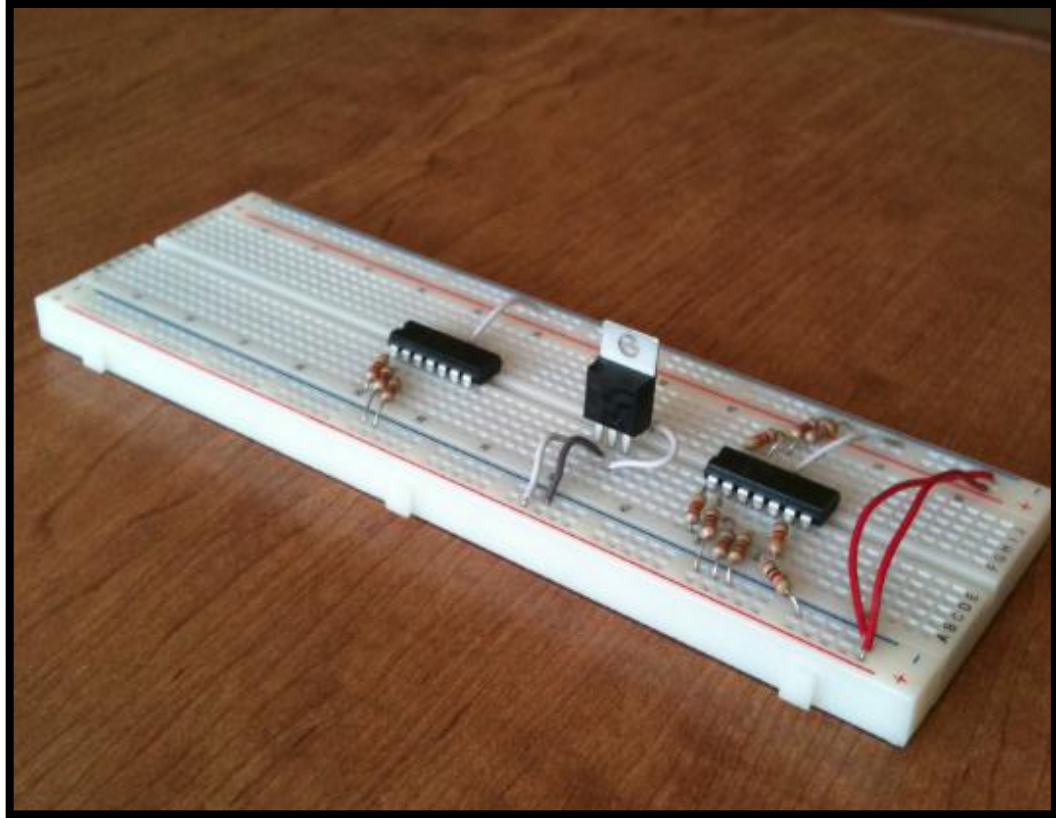


Figure 11: Side view of assembly step 2 for bread board circuit configuration

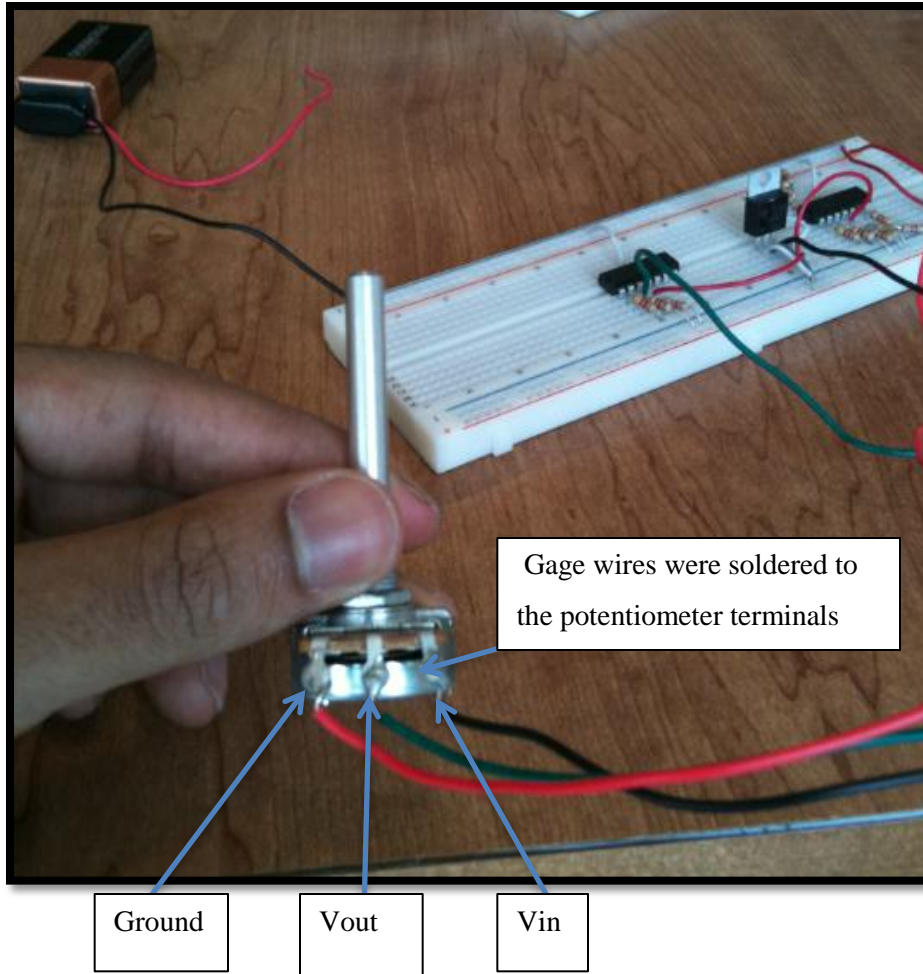


Figure 12: Assembly step 3 for bread board circuit configuration

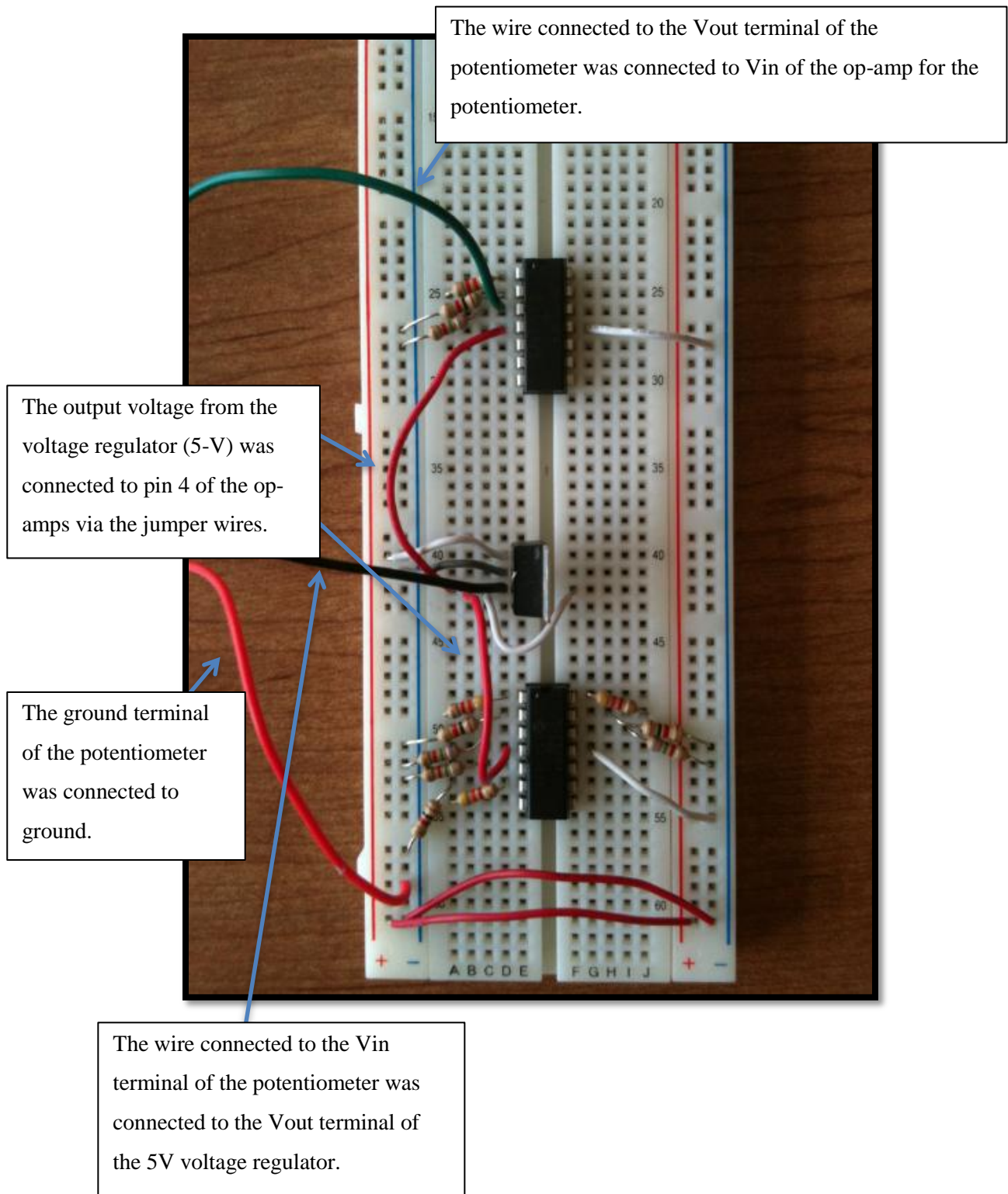
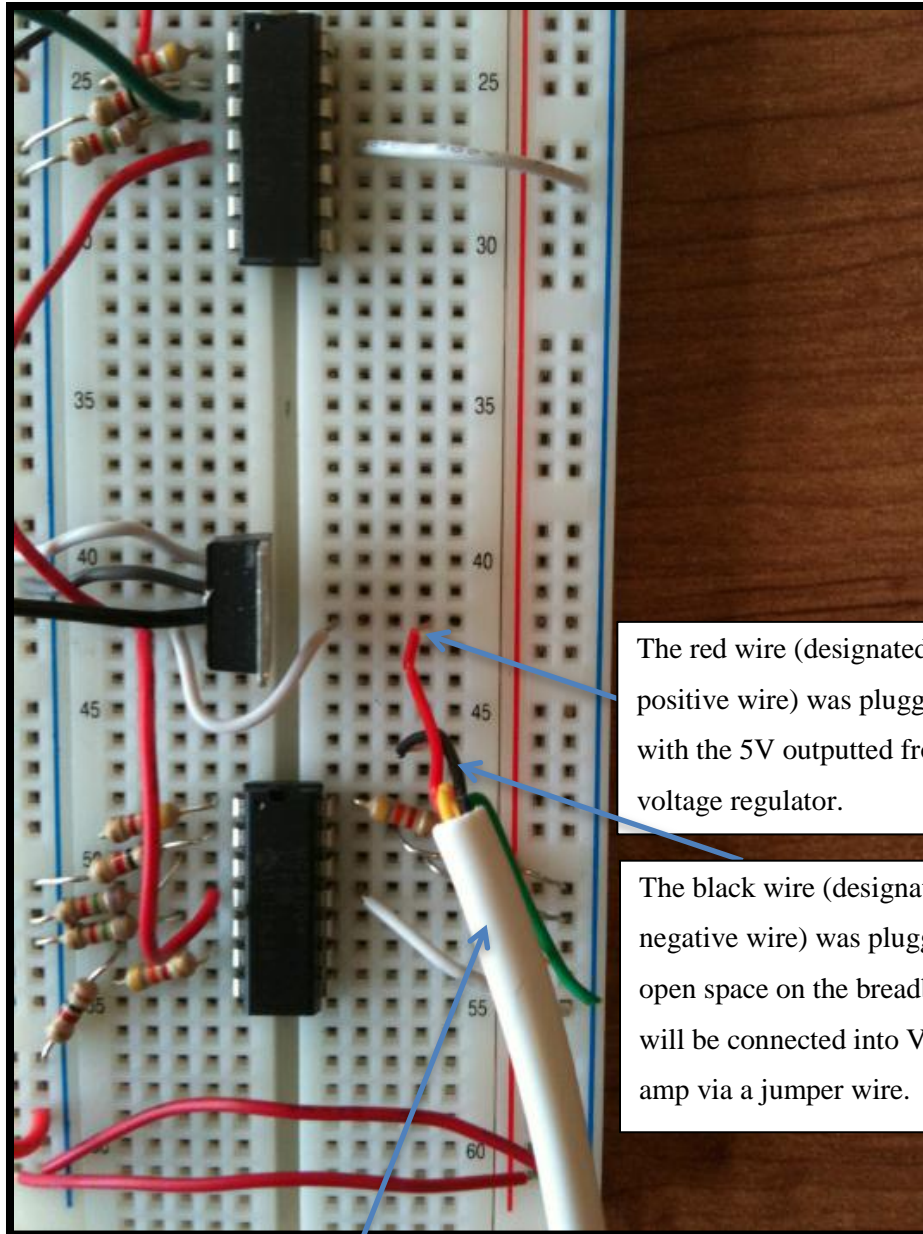


Figure 13: Assembly step 4 for bread board circuit configuration

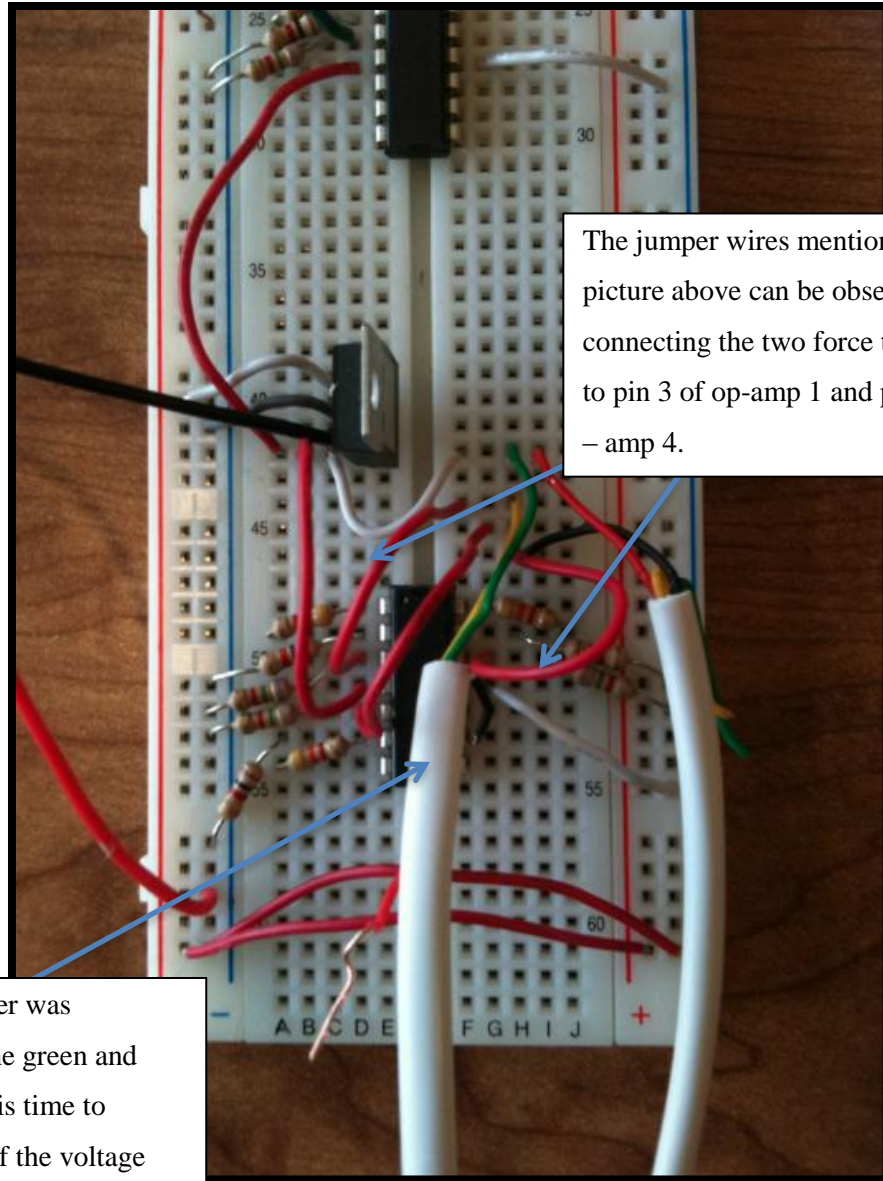


The red wire (designated as the positive wire) was plugged in series with the 5V outputted from the voltage regulator.

The black wire (designated as the negative wire) was plugged into open space on the breadboard. It will be connected into Vin of the op-amp via a jumper wire.

Gage wire was used to connect the force transducers to the breadboard, in which 4 wires are encased in the white wire coating.

Figure 14: Assembly step 5 for bread board circuit configuration



The jumper wires mentioned in the picture above can be observed here, connecting the two force transducers to pin 3 of op-amp 1 and pin 12 of op – amp 4.

The second force transducer was connected to op-amp 4. The green and yellow wired were used this time to connect to the 5V output of the voltage regulator and the Vin terminal of the op-amp respectively.

Figure 15: Assembly step 6 for bread board circuit configuration

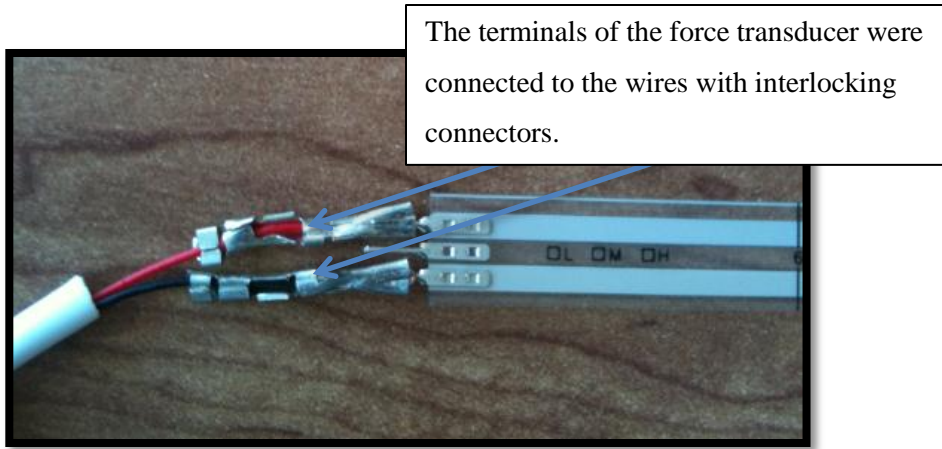


Figure 16: Assembly step 7 for bread board circuit configuration

The same wire used for the force transducers was used to connect the potentiometer and force transducers to the DAQ Box.

To avoid confusion, the yellow and green wires here are not being used for anything here. They are just bent back along the white coating.

The red wire was connected to pin 1 (Vout of op-amp 1). The black wire was connected to ground.

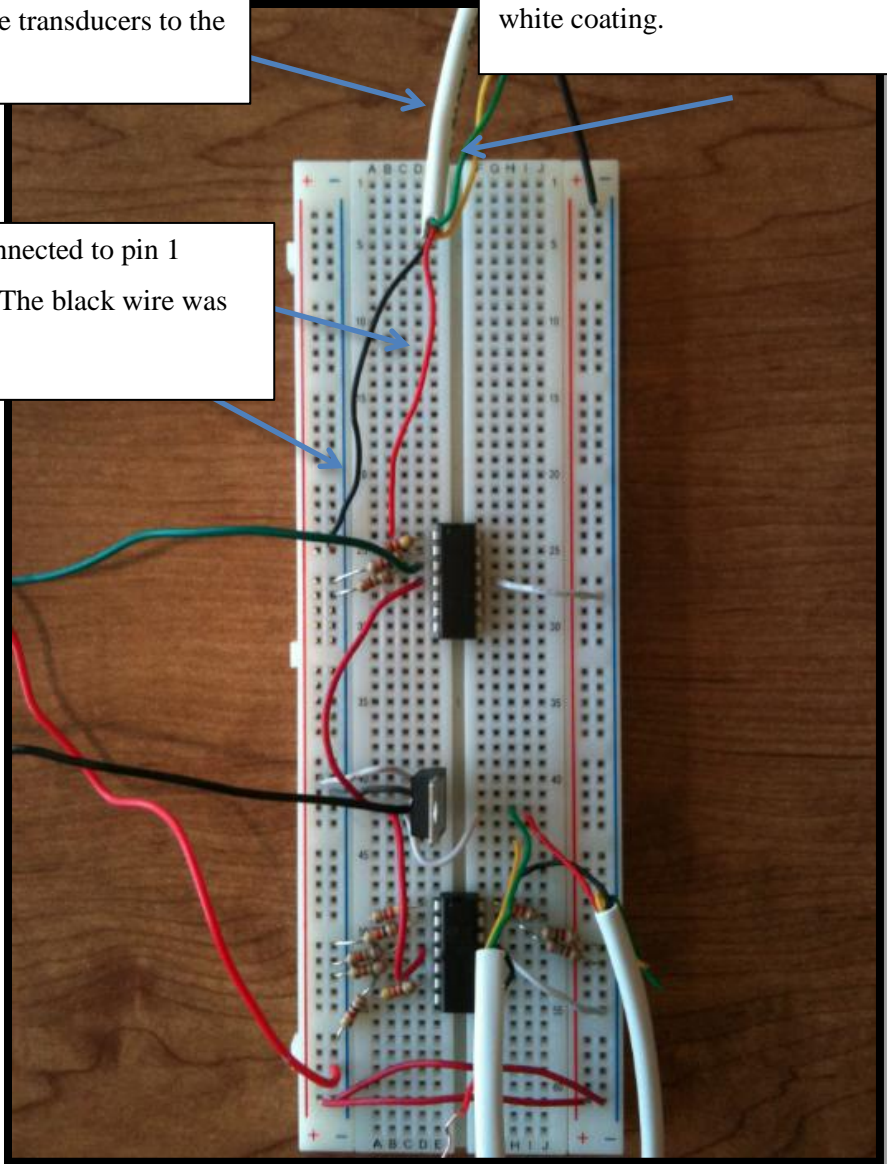


Figure 17: Assembly step 8 for bread board circuit configuration

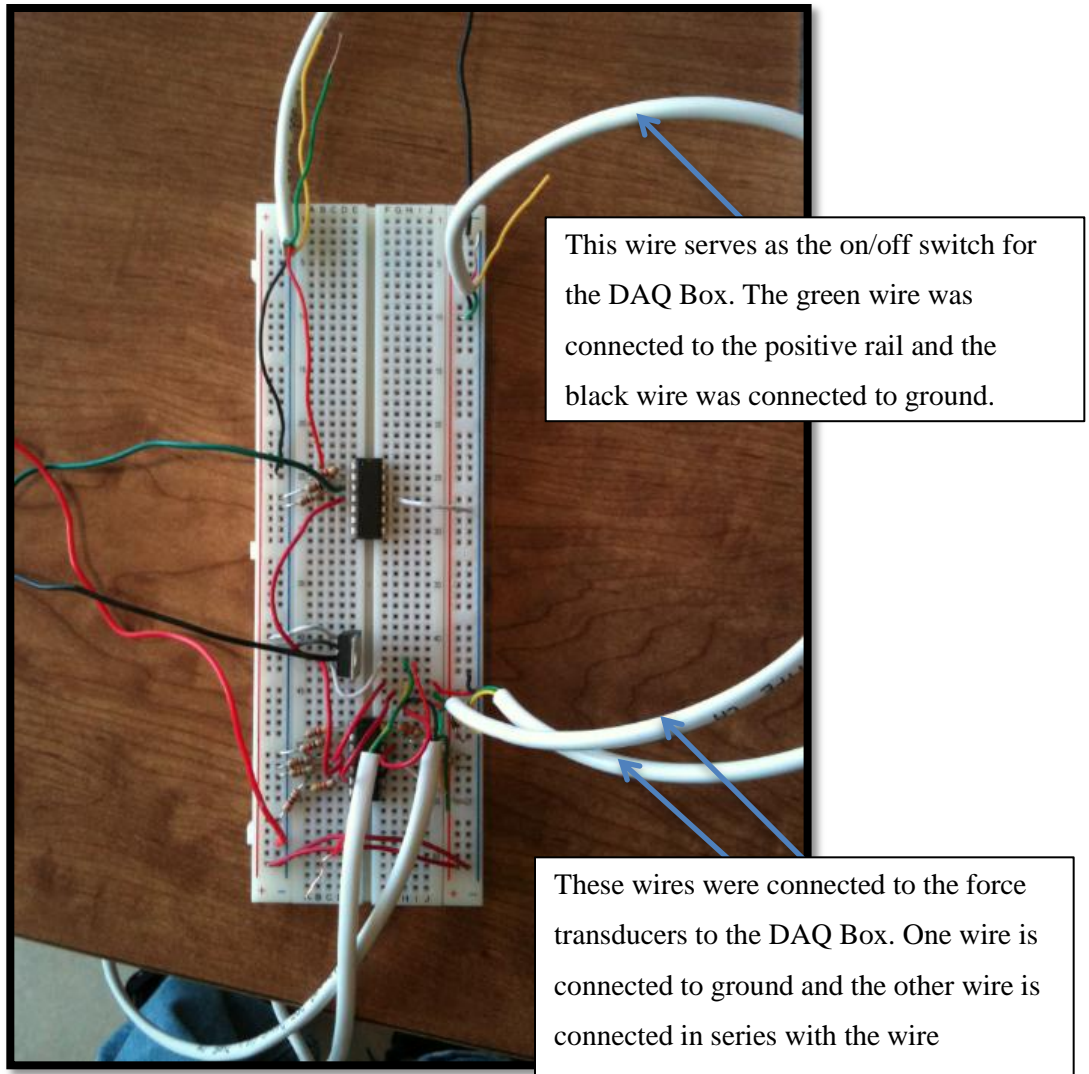
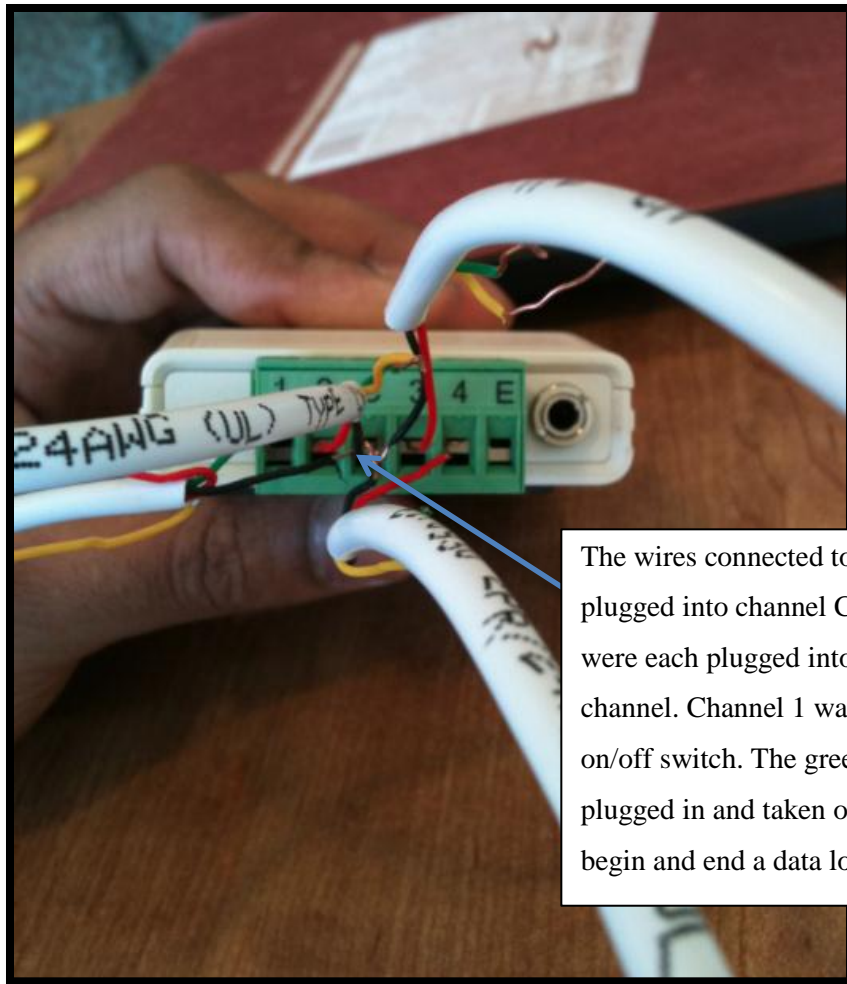


Figure 18: Assembly step 9 for bread board circuit configuration



The wires connected to ground were plugged into channel C. The other wires were each plugged into a designated channel. Channel 1 was used for the on/off switch. The green wire was simply plugged in and taken out of channel 1 to begin and end a data logging session.

Figure 19: Assembly step 10 for bread board circuit configuration

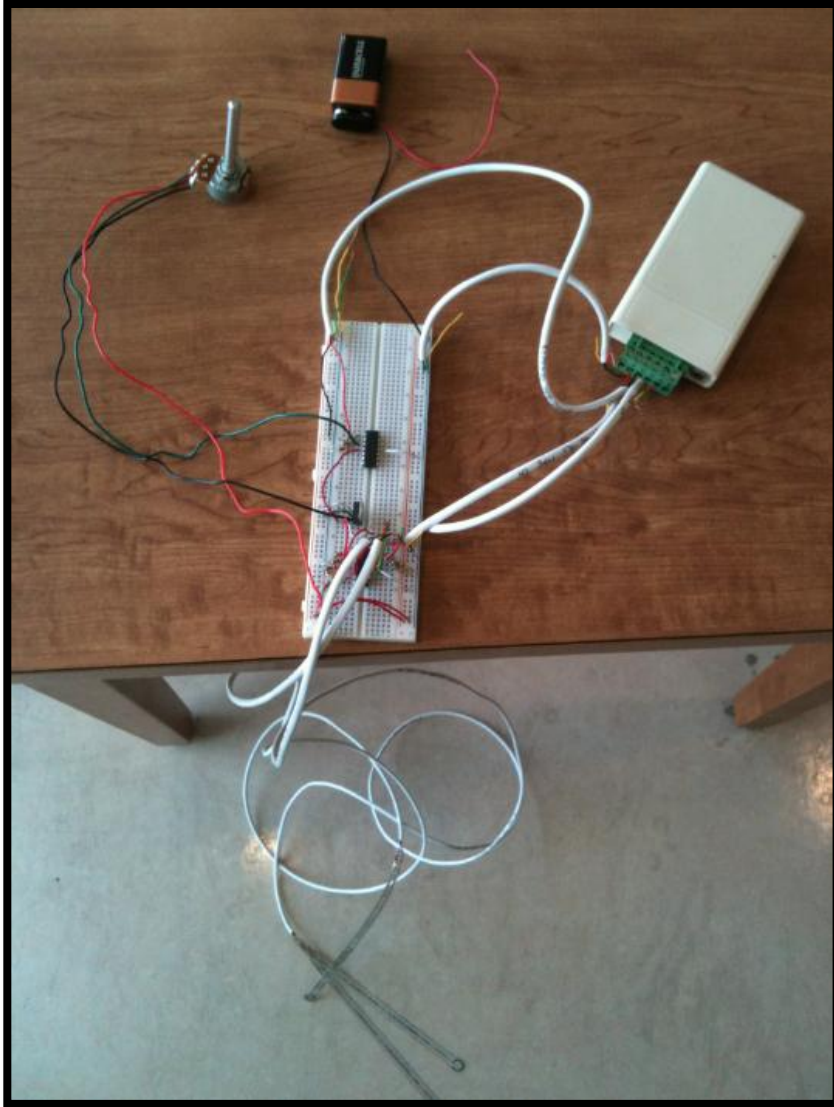


Figure 20: Final assembly step 11 for bread board circuit configuration, all components wired.

7. Methodology

There were three distinct ways that measurements were gathered throughout this experiment. The first was using force transducers on the feet. The force transducers measured the ground impact forces on the foot while in gait. The next device used in this experiment was a spinal rotation device, which measured the angle of spinal rotation while the test subject was in gait. The final method of data collection was through video analysis, which allowed accelerations to be calculated by placing tracking markers on the center of mass of the foot, shank, and thigh. The limb accelerations along with the flexion angles of the limbs were needed to solve for the forces in the ankle and knee joints. This study tested subjects as they were in jogging gait based on a specific guideline. The procedure and guidelines that the study followed are explained in detail in the following sections.

7.1 Force Transducers

After looking into several different methods of force measurement techniques, the group decided upon using force transducers as the method to measure the impact loads on the foot. The forces were obtained when the foot made contact with the ground when jogging. Since the main goal of this project was to investigate the forces that are exerted on the foot by the ground and correlate that force to the degree of spinal rotation when jogging in normal, exaggerated, and restricted form, only two force transducers were positioned on the heel of an insole in the right shoe. The number of force transducers placed in each shoe was limited by the number of input channels available in the data logger; however, it was determined that two sensors would be sufficient. The force transducers were placed where the largest pressures were typically experienced during the heel strike of jogging. These exact points were decided upon by using previous studies measuring the center of pressure. The image below shows exactly where the force transducers were placed on the foot.



Figure 21: Image of a pair of feet and exactly where the force transducers were placed on the right heel (indicated by the black dots)

The force transducers that were used throughout testing were TekScan FlexiForce A201 Force Transducers, which have a sensing area of 0.375 inches (9.53 mm) and the ability to measure weight up to 1000 pounds. The transducers were placed on the heel of the insole inside the right running shoe of the subject. They were wired to a breadboard and the output voltage was stored on a Pace Scientific XR440 Pocket Logger, where the data was available for analysis at any time.

The concept behind the force transducers on the foot was, upon ground impact the sensor readings would correlate to the overall force experienced upon landing during gait (jogging). This data was then to be used in a computational biomechanics analysis, which would allow for resulting forces in the ankle and knee joints to be determined.

7.2 Spinal Rotation

The spinal rotation device measured the change in voltage based on the rotation of the potentiometer, the rotation was driven by the rotation of the spine and shoulders while running with a normal, exaggerated, and restricted form. The resulting motion caused the potentiometer stem to rotate in a clockwise or counterclockwise direction, which changed the resistance of the potentiometer. With a change in resistance came a change in current respectively, which was measured and recorded using the Pace Scientific

XR440 portable data logger. The device was attached to the subjects using Velcro straps, which allowed for adjustable sizing and comfort while keeping it centered on the back. The spinal rotation device was positioned between the T1 and T12 vertebra, which is an area of the spine where a large amount of spinal rotation occurs for gait and movement.

The spinal rotation device was composed of an upper and lower spinal rotation portion. Each portion was a five inches long, one-inch in diameter wooden dowel in the vertical direction, connected by a 100kOhm linear taper potentiometer. The potentiometer was secured to the top of the lower dowel and then inserted into a pre-drilled hole in the upper dowel and secured. On each dowel, an aluminum bar (12"x2.5"x0.032") was placed horizontally and secured. A Velcro strap was then attached to each aluminum bar to allow the device to be firmly but comfortably secured to the subject for testing. The DAQ Box and breadboard for the force transducers and potentiometer were inserted in a fanny pack and strapped to the waist of each subject. This can be seen in the figure below.

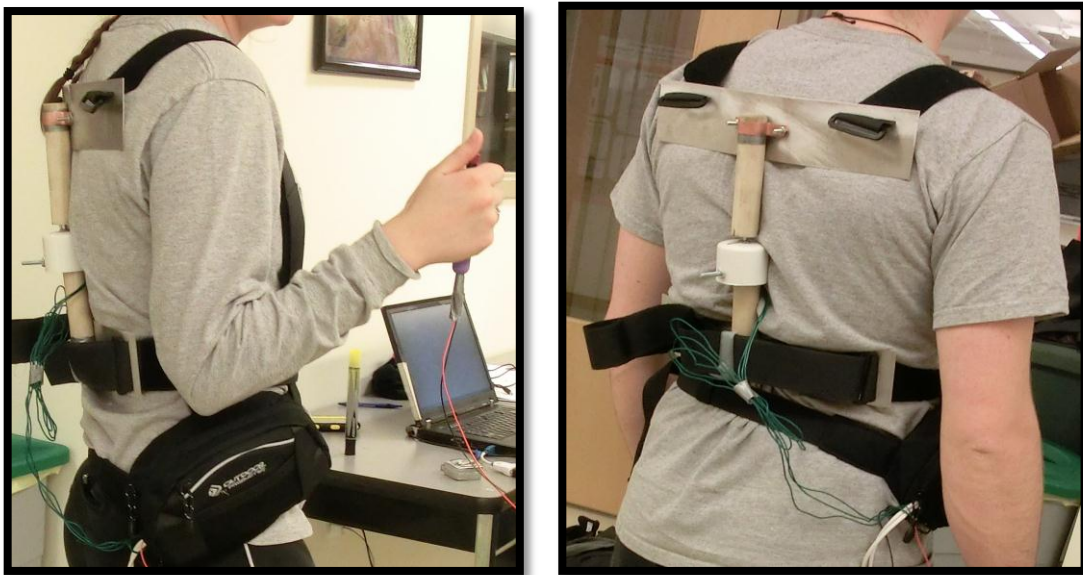


Figure 22: Spinal Rotation Device with Fanny Pack on a Female (to the left) and Male (to the right) Subject; shown from side angle and from behind

7.3 Video Analysis

In order to calculate changes in velocity and acceleration for each body segment, a high speed, wide-angle video camera was used. A Casio Ex-ZR100 camera, which allowed 240 frames per second to be captured, and a tripod were used to record the subject's gait

cycle. Tracking markers were placed on the subject's center of mass of their foot, shank, and thigh.

After equipped with tracking markers, they were filmed in a jogging cycle under normal running form, exaggerated spinal form, and restricted spinal form. The videos were exported to Adobe AfterEffects, which allowed for simultaneous motion tracking on the foot, shank, and thigh to be exported exportation directly to a spreadsheet. This provided the position of each point in each frame to be found. Using a known distance on the still frame and converting it to pixels, the velocities and accelerations were ultimately calculated.



Figure 23: Stationary image of subject with Trackers on the Center of Masses (to the left); Still shot image, tracking of subject while in jogging gait (to the right)

7.4 Testing Procedure

A Pace Scientific XR440 Pocket Logger and Pocket Logger software were used for recording the data from the force transducers and spinal rotation device during testing. The testing procedure relied heavily on the foot transducers acquiring the ground reaction forces. The project used an insole that was placed in the test subject's shoe, which

consisted of two FlexiForce A201 transducers placed on the heel for gait in the right shoe of each subject. The test subjects were assisted in putting on the equipment. Subjects had measurements of their upper and lower leg taken in order to properly locate the center of mass locations and were marked using tracking markers.

Each subject was allowed time to become acquainted with the spinal rotation device, insole, and testing procedures. The subject's normal running gait was monitored over a 20 meter distance; the data was then downloaded and saved to a laptop. The subject was then asked to run with exaggerated spinal rotation, using mainly their arms and spinal twist to drive their stride; the data was again downloaded and saved to a laptop. Lastly the subject was asked to run with restricting spinal rotation, but was told to not intentionally change anything other running mechanics, such as speed or stride length. After this trial the data was downloaded again. Before each trial the subject was asked to push down and hold the on/off button and when data was ready to be recorded to release the button. When each test was done the subject was instructed to click the on/off button to stop the data recording. After each trial the data was checked using a visual test in order to ensure the general expectation of each graph was met. If the general expectation was met the subject moved on to the next trial but if it was not met then the subject was asked to go through the test again. This method was repeated for all three running methods.

A more detailed testing procedure is included below:

- ☐ Methodology
 - Pre-Procedure
 - Notification to participant
 - Reserve 30 minutes for testing procedure
 - Wear comfortable athletic attire (running shoes, shorts/sweat pants, fitted shirt)
 - Equipment list
 - 2 FlexiForce transducers attached to insole
 - Fanny Pack
 - Pace Scientific XR440 Pocket Logger

- Breadboard
 - On/Off Button
 - Laptop Computer with Pocket Logger software
 - Spinal Rotation Device
 - Athletic tape and marker (for tracking markers)
 - Casio Ex-ZR100 camera and tripod
- Pre-test procedure
 - Description of testing procedure
 - Instructions on how to use On/Off button
 - Have participant fill out testing form and sign waiver
 - Take measurements
 - Attach tracking markers at center of mass locations on foot, shank, and thigh (athletic tape marked with a “X”)
 - Once insole is placed in right shoe, spinal rotation device attached using Velcro straps and aid of experimenters
- Running Test Procedure
 - Start data logger and camera recording
 - Run at a constant pace, release On/Off button
 - Subject runs 20 meters with normal rotation past the camera and clicks On/Off button
 - Walk back to start and experimenter downloads data from data logger onto laptop
 - Subject runs 20 meters run with exaggerated spinal rotation, clicks button and walks back to experimenter for data download
 - Subject runs 20 meters run with restricted spinal rotation, clicks button and walks back to experimenter for data download

- Post-procedure
 - Safely remove entire device
 - Calibration

In order to ensure that the potentiometer and force transducers values recorded during testing could be determined and converted from voltage to degrees and pressure respectively, the components were calibrated.

7.5 Potentiometer

- Voltage output, how does it compare with degree of rotation
- Express accurate data for the correlation of the spinal rotation of participant to their impact forces of the feet while actively jogging

7.5.1 Tools used

1. Tape
 - a. Hold down potentiometer
 - b. Hold down protractor
 - c. Attach metal indicator to the potentiometer stem
2. Indicator for gauge
 - a. Measure degree of rotation as stem turned (starting at 90 degrees)
3. Multi Meter
 - a. Measured voltage output from potentiometer
4. Computer
 - a. Find trend line to use the measured results to determine the degree of spinal rotation during testing
5. Breadboard
 - a. Connected to potentiometer and Multi Meter to measure the voltage output and act as a mediator
6. 9-V Battery
 - a. Power source

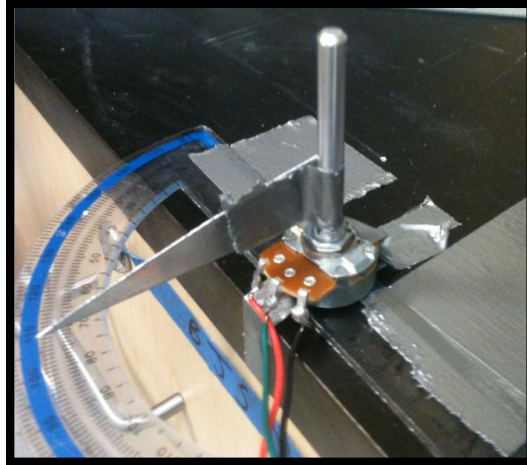


Figure 24: Process of Potentiometer Calibration

7.5.2 Process

1. Attached, with tape, the protractor to the outer edge of the table
2. Attached, with tape, the metal “needle” perpendicular to the potentiometer and parallel to the protractor to be used as an indicator for our gauge. This gauge measured the degree of rotation that we set the potentiometer to.
3. Attached, with tape, the potentiometer to the base of the protractor where 90 degrees of the protractor is 0 degrees of rotation.
4. The potentiometer was hooked up to the Multi Meter. The Multi Meter was used to display the voltage at the indicated degree of rotation.
5. The Multi Meter was set to 2.5V as the origin of our calibration. This means that when the gauge indicator read 90 degrees on the protractor, 0 degrees from the origin, the Multi Meter read 2.5V
6. The metal indicator was moved at increments of 5 degrees recording the voltage read out at every increment. This was done twice in both the negative and positive direction
 - a. The actual measurement of -5 and 5 degrees could not be recorded due to the fact the protractor did not display the measurement
7. All data was entered into Microsoft excel which then calculated the average and standard deviation

8. The data was then focused from negative -45 to 45 degrees, this was because any runner exceeding these measurements will be considered an outlier

Table 2: Calibration of Potentiometer Data

Degree	Voltage 1	Voltage 2	Average	Standard Deviation
-45	1.41	1.37	1.39	0.028284271
-40	1.56	1.53	1.545	0.021213203
-35	1.72	1.66	1.69	0.042426407
-30	1.81	1.76	1.785	0.035355339
-25	1.94	1.9	1.92	0.028284271
-20	2.05	2	2.025	0.035355339
-15	2.18	2.1	2.14	0.056568542
-10	2.3	2.25	2.275	0.035355339
0	2.5	2.49	2.495	0.007071068
10	2.73	2.7	2.715	0.021213203
15	2.86	2.8	2.83	0.042426407
20	2.98	2.94	2.96	0.028284271
25	3.14	3.08	3.11	0.042426407
30	3.29	3.21	3.25	0.056568542
35	3.46	3.38	3.42	0.056568542
40	3.63	3.57	3.6	0.042426407
45	3.83	3.77	3.8	0.042426407

9. A scattered plot was made from this data
10. A line of best linear fit was recorded from this data
11. The formula used to fit this trend line will be used during testing to determine the degree of rotation based on the output voltage of the potentiometer

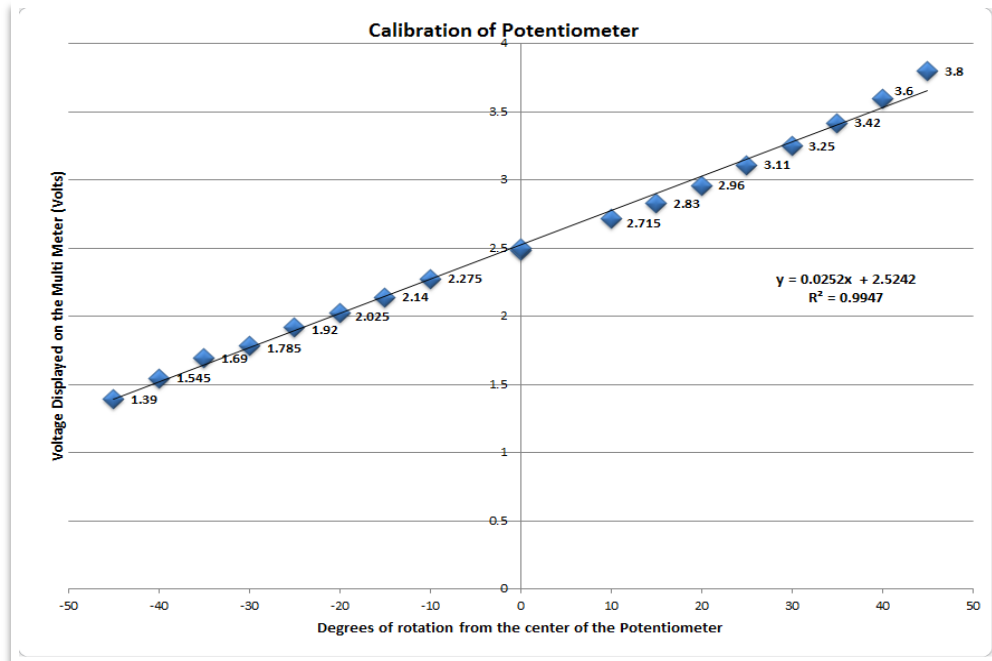


Figure 25: Potentiometer Calibration measured volts from -45 to 45 degrees where 5 degree increments were recorded. (Excluding -5 and 5 degrees)

7.6 Force Transducer Calibration

The group calibrated each force transducer used in the project in order to ensure the values received during testing were consistent with one another over the duration of the test period. To calibrate the force transducers the group used a static calibration method.

The static calibration method consisted of hanging a 2.27kg, 4.54 kg, 6.81 kg, and a 9.08 kg weight on a one-inch wooden dowel, which was placed directly on top of the force sensing area of the transducer (AS SHOWN BELOW). The transducers were wired into the breadboard with the output voltage being read directly on a voltmeter. The corresponding values for each weight was taken three individual times and then averaged. The average voltage was then plotted on a graph to show the voltage reading versus the known pressures.

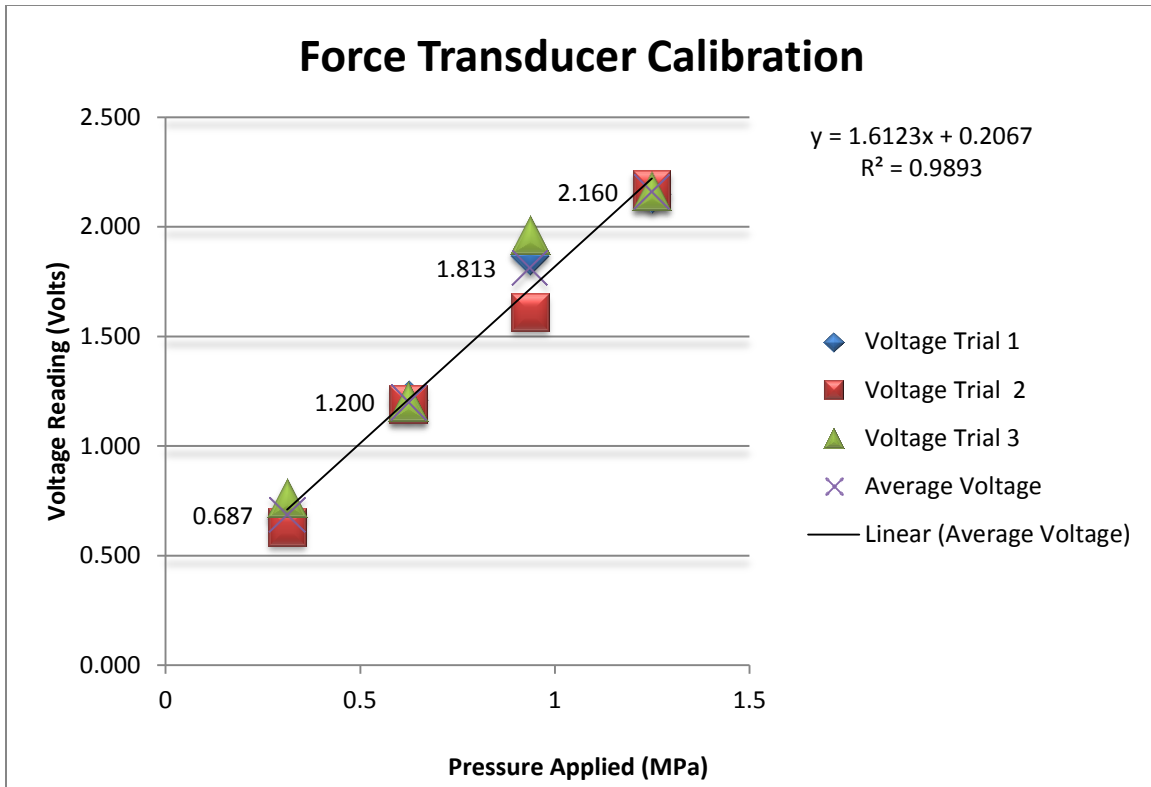


Figure 26: Calibration Curve of Force Transducer



Figure 27: Calibration of Force Transducer using a weight anchored directly on the sensing area of the Force Transducer

8. Results

This study consisted of testing twenty male and twenty female subjects while jogging normally, with exaggerated spinal rotation, and with restricted spinal rotation. The average age of all the test subjects was 20.1 ± 1.3 years (range, 18-22 years), the average weight was 66.9 ± 8.9 kg (range, 58.1-92.9 kg), and the average weekly mileage ran was 15 ± 4.7 km (range, 0-60 miles). The data collected was voltage readings for the spinal rotation and force transducers from the DAQ box as well as video that recorded the gait cycle. Video was used to track markers places at the center of masses of the foot and shank. These markers were used to measure angles and displacements as a means of calculating parameters such as velocities and accelerations of the lower leg and foot during gait.

8.1 Force Transducer and Spinal Rotation Results

The two force transducers were placed at the center of pressure locations on the heel by means of a shoe insert for the right shoe. A visual of the force output plots of spinal rotation and force transducers 1 and 2 can be seen below in Figure 28. As the figure illustrates, several different gait cycles were tested and implemented in this preliminary trial run. The voltage outputs for the potentiometer and force transducers were converted to degree of spinal rotation and force measurements respectively using the calibration curves.

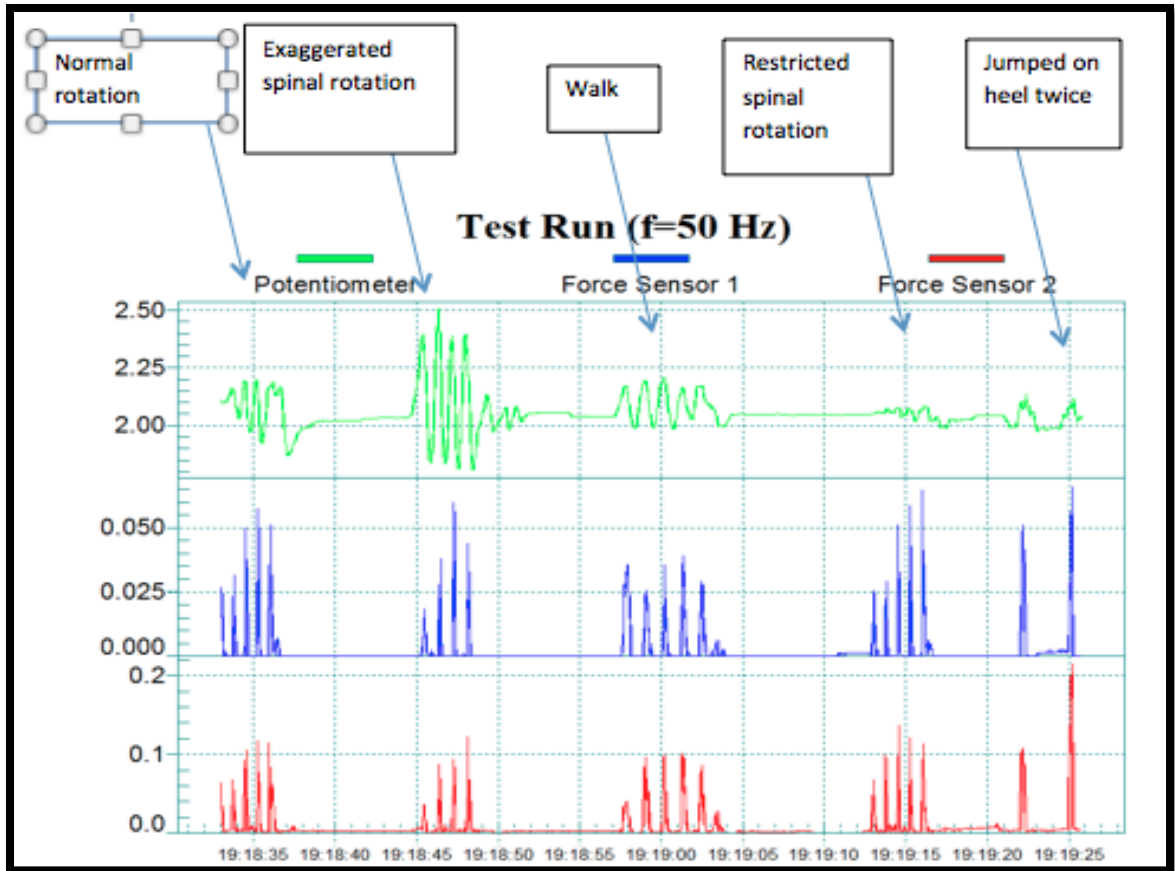


Figure 28: Visual of recorded data from DAQ box using Pocket Logger XR440 software.

The voltage readings showed an expected trend in which the amplitudes of the potentiometer waves increased with increased spinal rotation. This initial data also showed that the average voltages recorded were smallest for exaggerated spinal rotation when compared to normal and restricted spinal rotation. This agreed with the group's hypothesis.

Spinal rotation was measured using the voltage change that was recorded by the pocket logger. Once the pocket logger information was downloaded after each test subjects' run, the data was input into Microsoft Excel for analysis. The raw data, seen in Figure 28, showed the voltage change over time based on the rotation of the spinal measurement device. The raw data was later analyzed using a calibration curve to give spinal rotation measurements in degrees instead of a voltage output. The voltage change observed displayed a harmonic wave during the gait cycle.

8.2 Video Results

Each test subject was recorded for each trial run that they performed. The camera recorded from 2.5 meters away to allow for a full 3-meter horizontal span to be recorded. This allowed the subject to run with a completely unrestricted gait, because it did not force the subject to run within a frame area. The wide angle that was achieved enabled a minimum of one full gait cycle to be captured. The videos were then loaded into Adobe AfterEffects for analysis.

8.2.1 Tracking

1. Imported data from the Casio EX-ZR100 video camera into Adobe After Effects
2. A meter was measured physical before testing, this meter was measured in pixels to determine a pixel to meter conversion
 - a. Meter stick was used throughout this section as a reference frame
3. Tracked the center of mass of the foot and knee by using digital markers that follow the physical markers placed on the subject for testing
4. Determined the fixed heel point of the subject according to the initial impact of the heel. This was measured in x and y pixels
5. The initial toe off of the previous foot was determined using the pixels
6. Stride length was determined by subtracting the toe off point from the following heel strike in pixels. This is because the entire picture is in the first coordinate system.
7. The pixel measurement of stride length was converted to meters by using the previous conversion.

8.2.2 Force and Knee Analysis

1. Transferred the feature center data to Excel from Adobe After Effects. This is the center of mass of the foot designated by the marker tracked.
2. **Track Point Feature Center:** Looked at and evaluated frames to determine which ones would be used for analysis. They were evaluated on the basis of when the

mass load is transferred to the ankle and knee from the foot. The data used is from the initial heel strike to when the motion of the foot begins to decelerate.

3. **Radius:** The assumption of the radius from the center of pressure to the center of mass increases as the foot decelerates due to the inverse pendulum theory on rigid bodies.

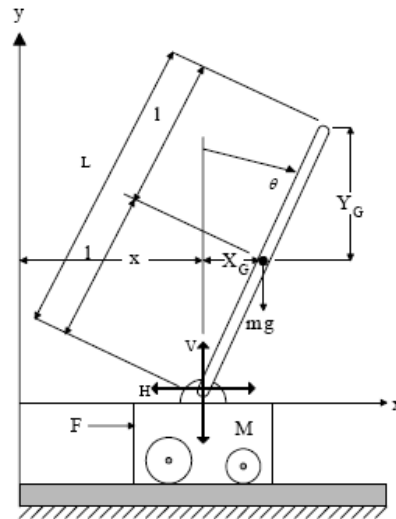


Figure 29: The Inverse Pendulum Theory

4. This was analyzed per frame from the initial heel strike with the Pythagorean Theorem measured in pixels.
5. Using the conversion factor found previously, the pixel measurement of the radius was converted to meters
6. **Angles:** The change in the x was calculated by subtracting the heel fixed point of x from the moving marker in each frame.
7. The change in y was calculated with the same process.
8. The angle was calculated by taking the arctangent of the change in y over the change in x measured in radians.
9. This calculation was then converted to degrees by multiplying the radians calculated by $180 / \pi$.
10. **Individual Angles:** Individual angle were determined by taking the difference of the foot angle over the past two frames.

11. This was measured in radians and converted to degrees in the same format as previously stated.
12. **Angular Velocity:** The angular velocity was evaluated by the individual angle calculated multiplied by the number of frames per second. 240 frames per second were used.
13. **Angular Acceleration:** The angular acceleration was calculated by finding the difference between the angular velocity between the past two frames and multiplying it by the rate of frames per second. "120 frames per second" was used because two frames were used.
14. **Alpha Tangent:** The angular acceleration (alpha tangent) was calculated by multiplying the angular acceleration by the radius of the foot in meters.
15. **Alpha Normal:** The radial acceleration (alpha normal) was calculated by multiplying the radius in meters by the angular velocity squared.

8.3 Force Plate Results

Four subjects were tested on the force plate while still wearing the spinal rotation device. 2-D musculoskeletal models from last year's MQP were used to analyze the forces acting on the lower extremities during gait. Figure 30 is a free body diagram of the foot. The segments analyzed were assumed to be rigid bodies, a common method used in biomechanics. To get the distance of the ankle to heel, the length from the end of the foot to the heel was subtracted by the length of the end of the foot to the ankle joint. The height of the ankle to heel was measured as a percentage of the length of the foot. The weight of the foot acts at the COM, so the distance to the ankle joint was needed. The length from the end of the foot to the COM, was subtracted by the length of the end of the foot. These distances are necessary to solve for the resulting moment in the ankle joint. The image shows the x and y components of the ground force in orange. This force vector acts at the center of pressure of the foot. To fit the model, the group studied subjects that landed with a heel strike form. In this form, the area of the center of pressure is smaller and focused on the calcaneus (heel bone). Three equations were used to solve for the

resulting forces and moments in the ankle joint. The three equations are shown below.

$$\sum F_Y = M_{ay} = F_{yNormal} - W_{foot} + F_{yResultant}$$

$$\sum F_X = M_{ax} = -F_{xNormal} + F_{xResultant}$$

$$\sum M_{ankle} = I(\alpha) = -F_{ynormal} * (D_{a_h}) - F_{xnormal} * (H_{a_h}) - W_{foot} * (D_{a_COM}) - M_{ankle}$$

In the three equations above, the x and y resultant forces were calculated along with the resultant moment in the ankle. These three values are used to solve for the muscle forces along with the compressive force in the bone. Translating the anatomy of the foot to a free body diagram was challenging because the anatomy is not representative of how the forces act on the rigid body. A combination of models found in literature and anatomy books were used to form the model. The distances from the ankle joint to the muscles were measured as a percentage of the foot length. The tibialis anterior angle was calculated using the angle of ankle flexion, the insertion point distance on the foot, the insertion point distance on the shank, and the law of cosines. Calculating these forces also needed to account for the angle of the rigid bodies, measured from the video recordings (2-D X,Y plane). The sum of the force and moment equations were set equal to zero because the resultant values already account for the dynamic variables. The three equations used are shown below.

$$\sum F_Y = 0 = F_{ta} * \sin((\text{angle}_{ta}) - (\text{angle}_{foot})) + F_{ach} * \sin((\text{angle}_{each}) - (\text{angle}_{leg})) - F_{B1} * \cos(\text{angle}_{leg}) + F_{RY}$$

$$\sum F_X = 0 = F_{ta} * \cos((\text{angle}_{ta}) - (\text{angle}_{foot})) - F_{ach} * \cos((\text{angle}_{each}) - (\text{angle}_{leg})) + F_{B1} * \sin(\text{angle}_{leg}) + F_{RX}$$

$$\sum M_{ankle} = 0 = F_{ta} * (\sin(\text{angle}_{ta})) * (D_{ta}) - F_{ach} * \sin((\text{angle}_{each})) * (D_{ach}) + M_{ankle}$$

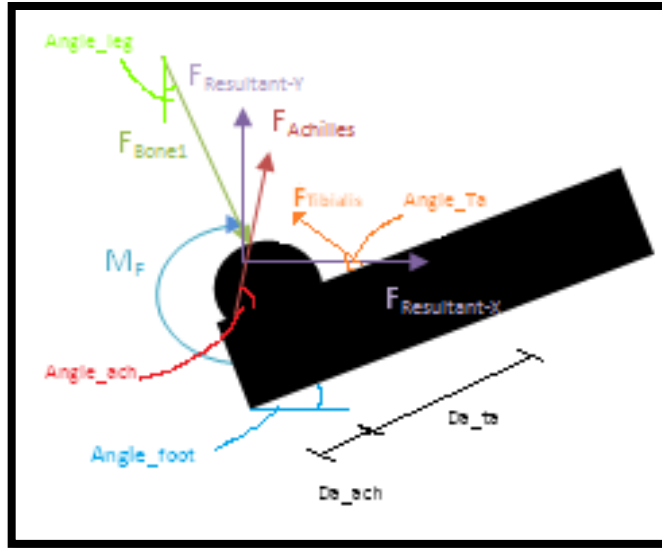


Figure 30: Free body diagram of the foot with muscles

MATLAB was used to solve the three unknown variables using matrix equations. These muscle and bone forces were then translated to the shank to solve for the hamstring, patella, and knee joint forces. The muscle vectors are always in tension and thus directed off of the rigid body. The joint force is compressive which is directed at the rigid body. When translating the vectors to the shank free body diagram, the magnitudes are equal, but the direction is opposite.

Figure 31 below is the free body diagram of the shank. The only external forces acting on this rigid body is the weight of the leg. The mass and acceleration is also accounted for in the equations below.

$$\sum F_Y = M a_y = -W_{\text{shank}} + F_{y\text{Resultant}}$$

$$\sum F_X = M a_x = F_{x\text{Resultant}}$$

$$\sum M_{\text{knee}} = I(\alpha) = -W_{\text{shank}}(D_{a_COM}) - M_{\text{knee}}$$

The forces that the knee joint experiences during impact are through the translation of the ankle joint force and the muscle forces. The Achilles tendon connects to two muscles, the soleus and gastrocnemius. The soleus inserts on the shank, where the gastrocnemius inserts just above the knee joint. These two muscles are fractions of the

total Achilles tendon force, the soleus (2/3) and the gastrocnemius (1/3). The insertion points of the hamstring, patella, tibialis, and soleus were found using the same method that was used in the foot. The angle of the hamstring was determined using the law of cosines based on the insertion point on the shank, thigh, and the angle of knee flexion. The soleus and patella angles were measured values. Below are the three equations used to solve for the unknown variables.

$$\sum F_Y = 0 = -F_{ta} \cdot \cos((\text{angle}_{ta}) + (\text{angle}_{leg})) - F_{sol} \cdot \cos((\text{angle}_{sol}) - (\text{angle}_{leg})) + F_{B1} \cdot \cos(\text{angle}_{leg}) + F_{RY} + F_{ham} \cdot \cos((\text{angle}_{ham}) + (\text{angle}_{leg})) + F_{pt} \cdot \cos((\text{angle}_{pt}) - (\text{angle}_{leg})) - F_{B2} \cdot \cos(\text{angle}_{high})$$

$$\sum F_X = 0 = -F_{ta} \cdot \sin((\text{angle}_{ta}) + (\text{angle}_{leg})) - F_{sol} \cdot \sin((\text{angle}_{sol}) - (\text{angle}_{leg})) + F_{B1} \cdot \sin(\text{angle}_{leg}) + F_{RX} - F_{ham} \cdot \sin((\text{angle}_{ham}) + (\text{angle}_{leg})) + F_{pt} \cdot \sin((\text{angle}_{pt}) - (\text{angle}_{leg})) + F_{B2} \cdot \cos(\text{angle}_{high})$$

$$\sum M_{knee} = 0 = F_{ta} \cdot \sin((\text{angle}_{ta})) \cdot D_{ta} - F_{sol} \cdot \sin((\text{angle}_{sol})) \cdot D_{sol} - F_{ham} \cdot \sin((\text{angle}_{ham})) \cdot D_{ham} + F_{pt} \cdot \sin((\text{angle}_{pt})) \cdot D_{pt} + M_{knee}$$

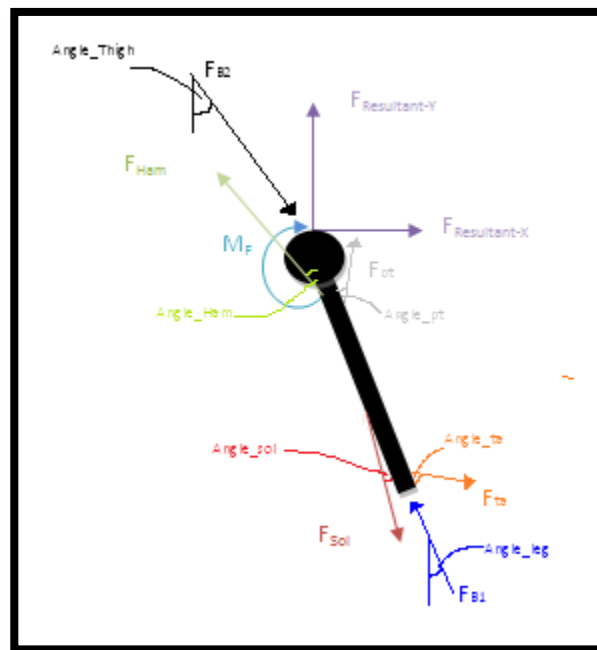


Figure 31: Free body diagram of the knee with muscles

9. Analysis

The initial analysis of the data took place in two stages: analysis of the voltage outputs from transducer and analysis of the video components. The voltage outputs were analyzed for both the degree of spinal rotation and forces experience in the heel during gait. They were analyzed by calibrating the transducers using known values to produce a curve, then applying the curve to the voltage outputs giving rotational and force measurements. The analysis of the video components took place using a combination of Adobe AfterEffects and Microsoft Excel. The analysis revealed the angles, distances, velocities, and accelerations of limbs that were required for the computational analysis of solving for forces.

Once the first two stages of analysis were completed, four subjects were called back to run a follow up test using the force plates to measure ground reaction forces. The first two stages of analysis allow for the third stage, in which a final computational analysis was used to solve for resultant forces experienced throughout the foot and knee during gait.

9.1 Voltage Output Analysis

Each subjects output voltages for the spinal rotation device and foot transducers were downloaded from the data logger after each trial run. The data was then saved into a text file so that excel could be used to read the resulting data. Once in Excel, the calibration curves were applied to the voltage outputs to give the degree of spinal rotation. For the force transducer data, the excel data was imported into MatLab, following the steps listed below:

1. Extract trial from Pocket Logger form to CSV file for Microsoft Excel
2. Inside Excel
 - a. Remove the "Date" section of the data in Column A
 - b. Remove all semicolons ":"
 - c. Insert a column into the data set next to the "millisecs" column named "Time (sec)"
 - i. Convert from milliseconds to seconds in the "Time (sec)" column

- d. Insert a column next to the “Ch3” and “Ch4” named “Ch3_Pressure(kPa)” and “Ch4_Pressure(kPa)” respectively
 - i. Convert from voltage readings in “Ch3” and “Ch4” column to pressure in “Ch3_Pressure(kPa)” and “Ch3_Pressure(kPa)” column respectively using the calibrations
- e. Save the Excel Spreadsheet
3. Open up MatLab program
 - a. Open up code in editor of MatLab
 - b. Edit code accordingly
 - c. Run the code
 - d. When the figure opens select which peaks from force transducer 1 that want to be included in study
 - i. Proper syntax for peaks is vector notation, for example [1 2 3 4 10 13]
 - e. After entering the peaks that are being used another figure will appear and again select which peaks from force transducer 2 that want to be included
 - f. Repeat process for all subjects
 - g. Then repeat the process for each type of test (exaggerated, normal, and restricted)
4. Copy and paste the data from MatLab (the ResAll information) to Microsoft Excel
5. Determine the correlation between spinal rotation and pressure

9.1.1 Force Transducer Output

After all the tests were complete for each subject, the force transducer data was analyzed. When studying the force transducer data, the group noticed that the force values compared to the calibrated force values were significantly low compared to literature values, which reported values up to 2 times body weight. When reviewing the video data for those subjects, it was noticed that, due to variations in running techniques and landing styles, that subjects landed with pronation, supination, or other variations of landing forms. This explains the lower recorded pressure values from the force transducers, as they were not placed in the most accurate location from subject to subject, so the maximum force experienced could not be measured. For this reason, the force transducer readings were unable to be used in further analysis where the group had hoped and this provoked the group to call back a few subjects to test on the force plate.

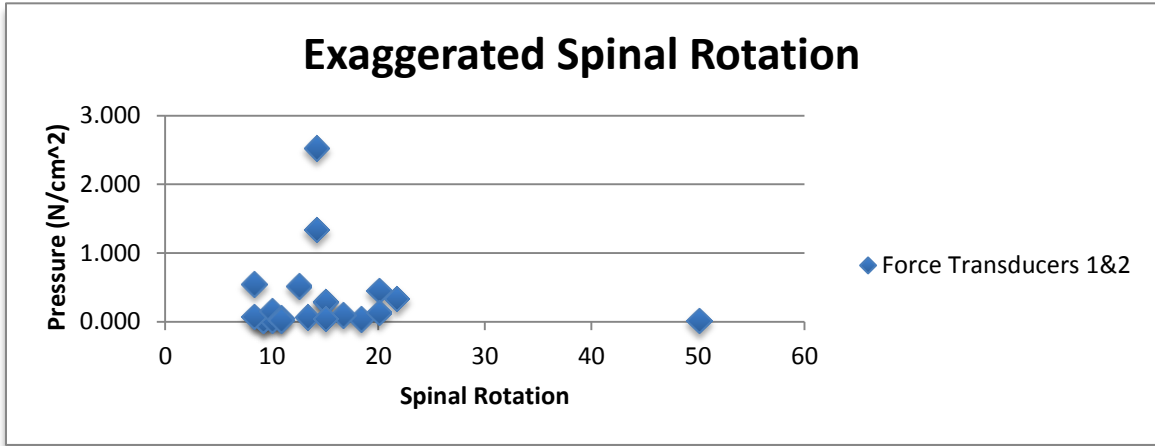


Figure 32: Plot of spinal rotation vs. pressure for exaggerated spinal rotation test.

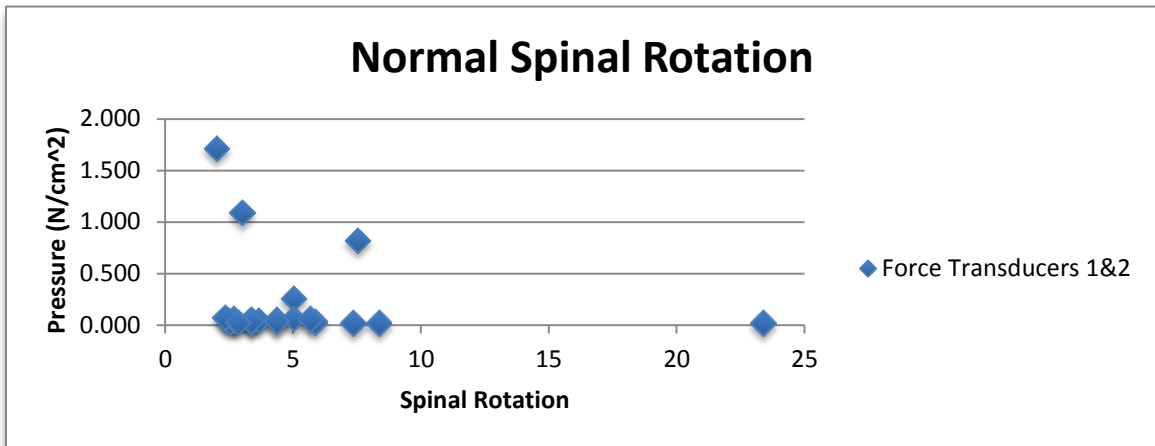


Figure 33: Plot of spinal rotation vs. pressure for normal spinal rotation test.

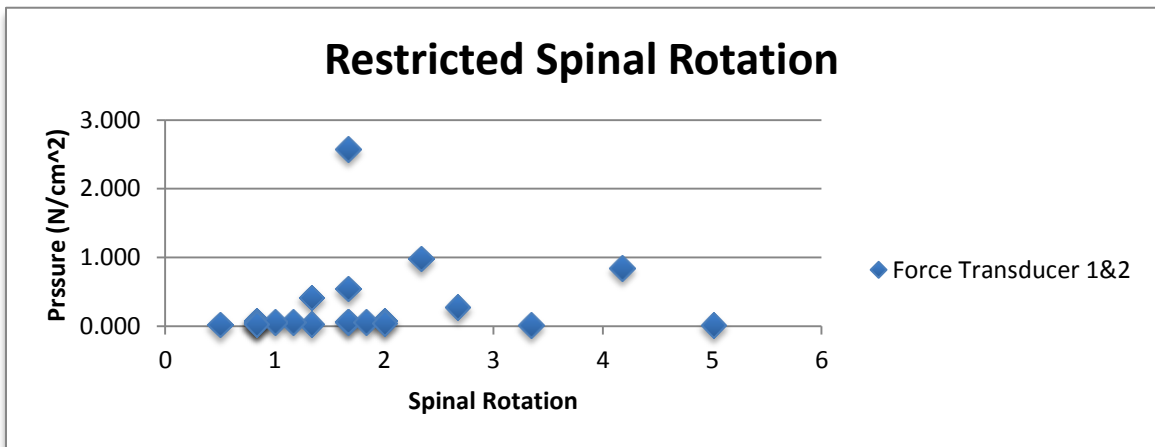


Figure 34: Plot of spinal rotation vs. pressure for restricted spinal rotation test.

The tabulated data can be viewed in Appendix E.

9.1.2 Spinal Output

The information recorded by the data logger was exported into Excel and then analyzed using the calibration data that was performed earlier. Spinal rotation measurements were taken for all three trials of the majority of subjects. Spinal rotation was determined by graphing the values in excel and calculating the degree of rotation from the midsagittal plane facing forward to the point at which full rotation was achieved. Subjects that were not recorded in the tables below did not run with a constant velocity relative to the other subjects, or landed in such a manner that little to no contact was made with the force transducers. Therefore their data was omitted. The average spinal rotation for a normal gait cycle was 5.2 +/- 4.7 degrees, exaggerated gait cycle was 15.4 +/- 9.1 degrees, and restricted was 1.8 +/- 1.2 degrees. The tabulated data can be viewed in Appendix F.

9.2 Video Analysis

Each video was analyzed separately using Adobe After Effects CS5 and the resulting values imported into Microsoft Excel for further analysis. The first part of the video analysis recorded the position of the tracking markers, in pixel location, during the impact of the foot during the gait cycle. Each marker was tracked separately and the corresponding pixel locations of the marker for each frame were exported into Excel.

Once in Excel, the pixel locations of the markers were identified by the frame number and the corresponding heel strike frames were analyzed. After the frames were chosen, the pixel locations for each frame were put into a formula that solved for angular velocity, angular acceleration, Cartesian velocity, and Cartesian acceleration.

The average acceleration in the x-direction and y-direction were the two values that were closely observed. The sensitivity of the data resulted in a range of accelerations for the nineteen subjects that were chosen for corresponding analysis. The participants were

then separated further into six subjects to be reanalyzed to ensure the pixel locations corresponded with an accurate location of the tracking marker. The result was accelerations that still were significantly different.

Foot impact angles were also calculated using Adobe After Effects CS5 as well. Other important angles were calculated using the positions of the tracking markers, specifically the angle of the tibia. In the following the analysis of the foot and knee will be explained further. Figures 7 through 14 below display the angular velocities and accelerations of the foot and knee for one test subject's normal rotation jog.

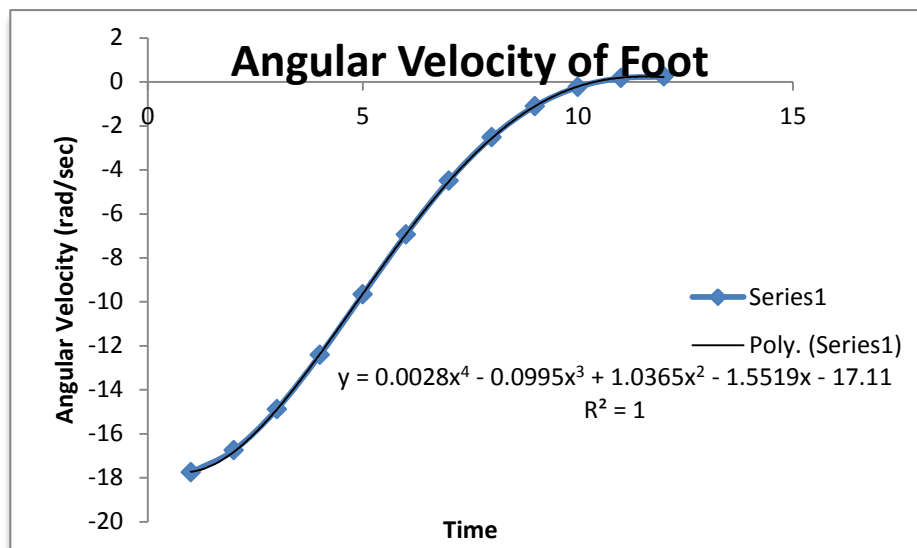


Figure 35: Angular velocity of the foot from heel strike to toe off

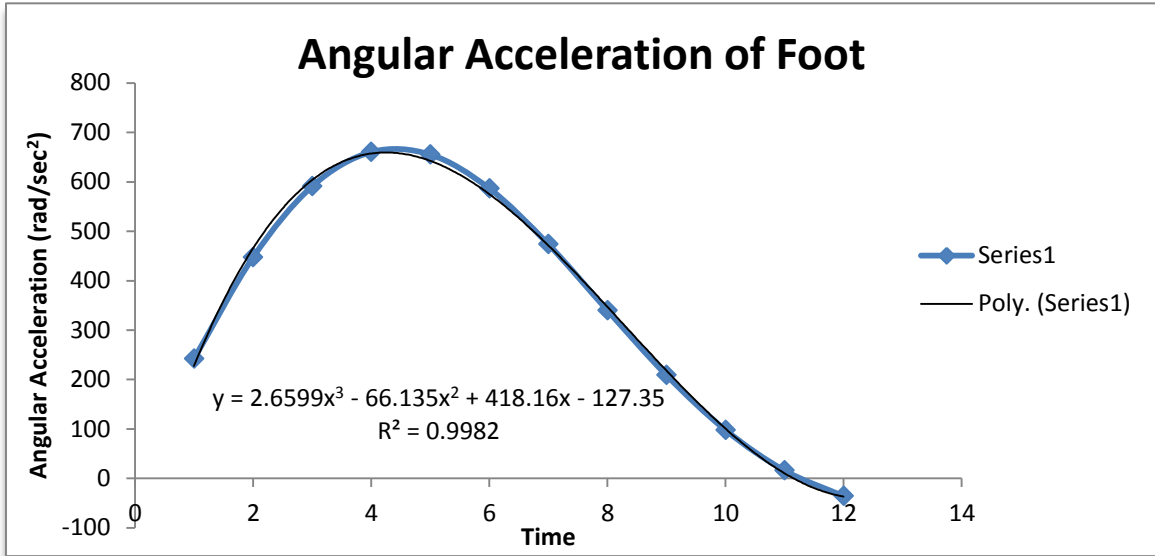


Figure 36: Angular acceleration of the foot from heel strike to toe off

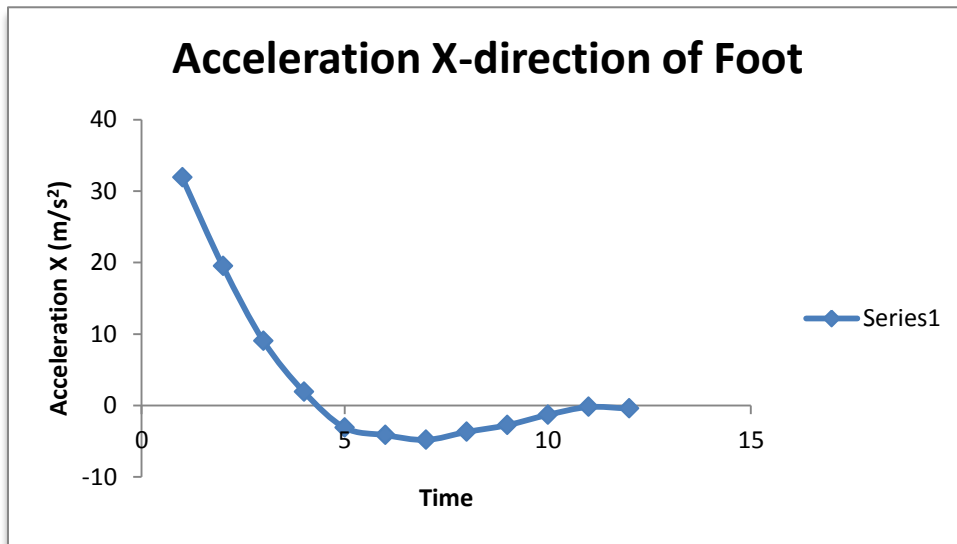


Figure 37: Acceleration in the x-direction of the foot from heel strike to toe off

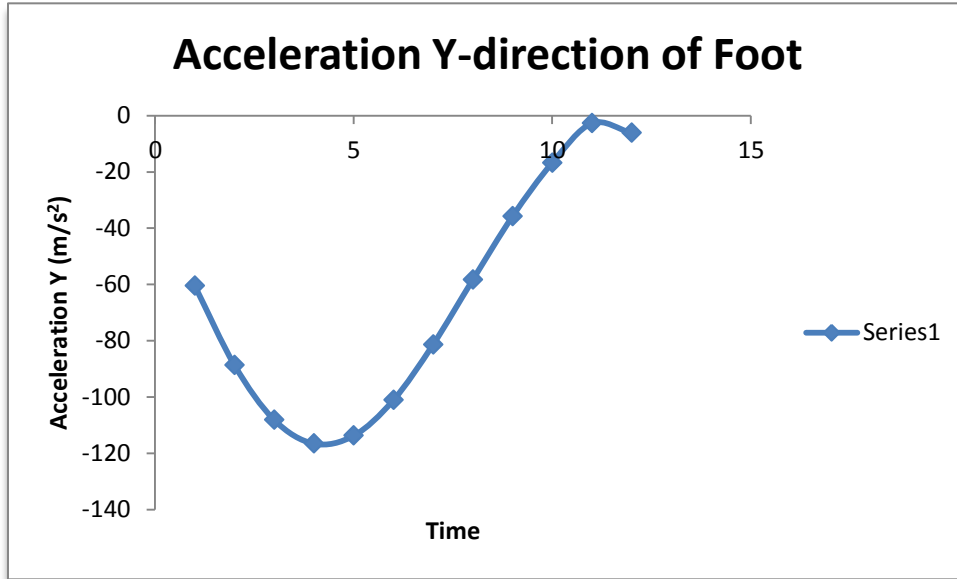


Figure 38: Acceleration in the y-direction of the foot from heel strike to toe off

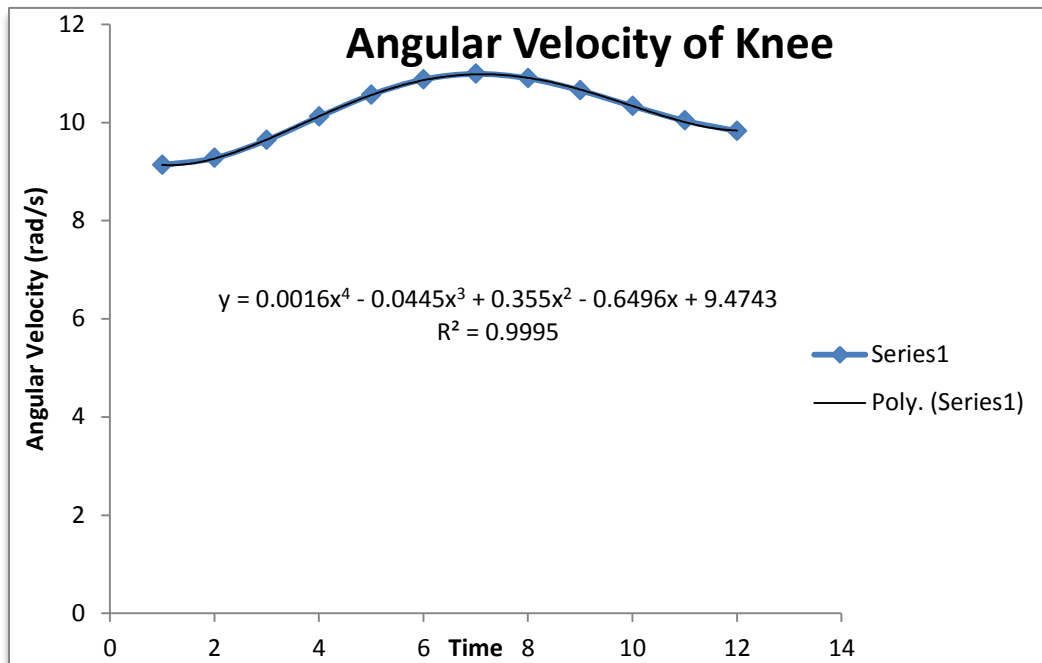


Figure 39: Angular velocity of the knee from heel strike to toe off of gait cycle

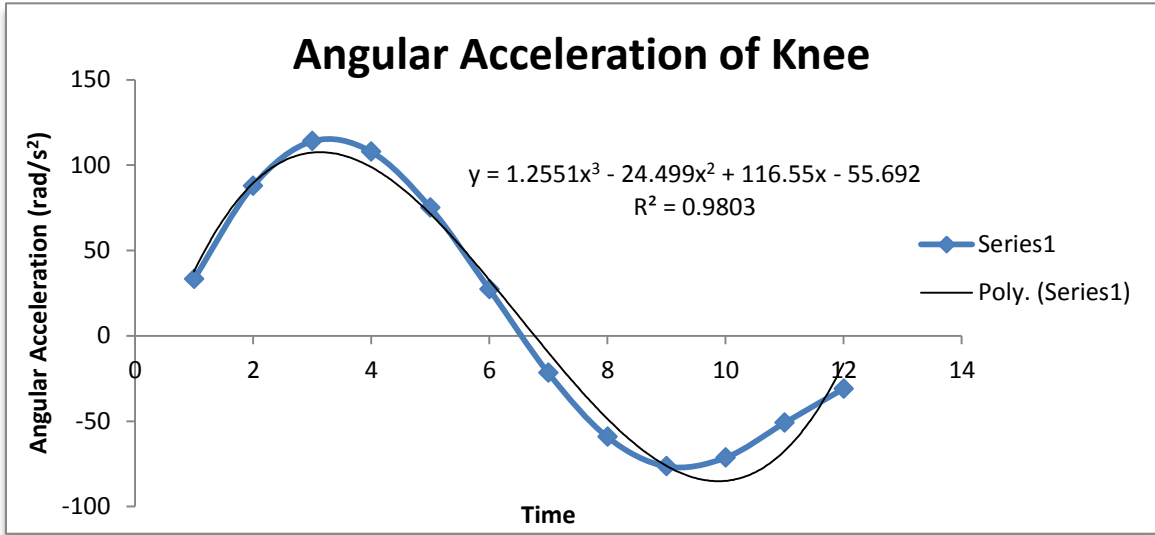


Figure 40: Angular acceleration of the knee from heel strike to toe off of gait cycle

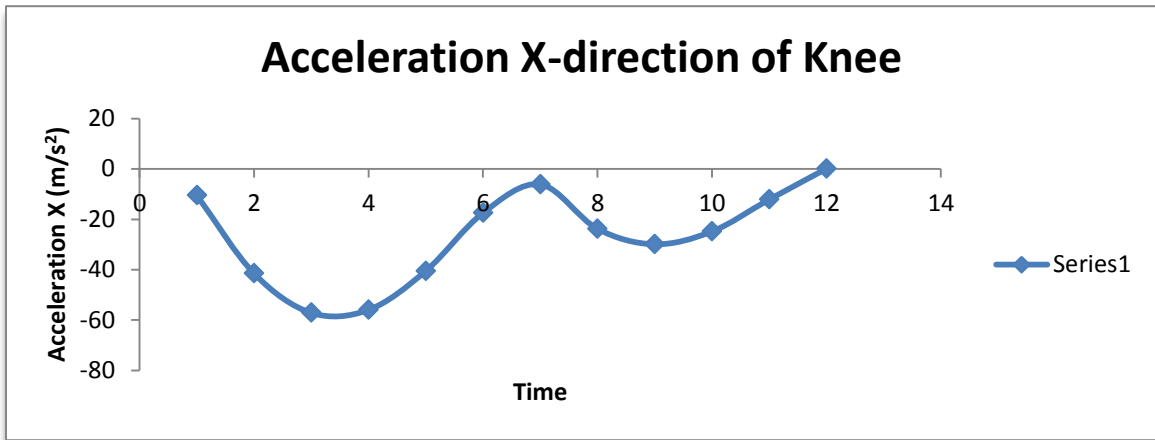


Figure 41: Acceleration in the x-direction of the knee from heel strike to toe off of the gait cycle

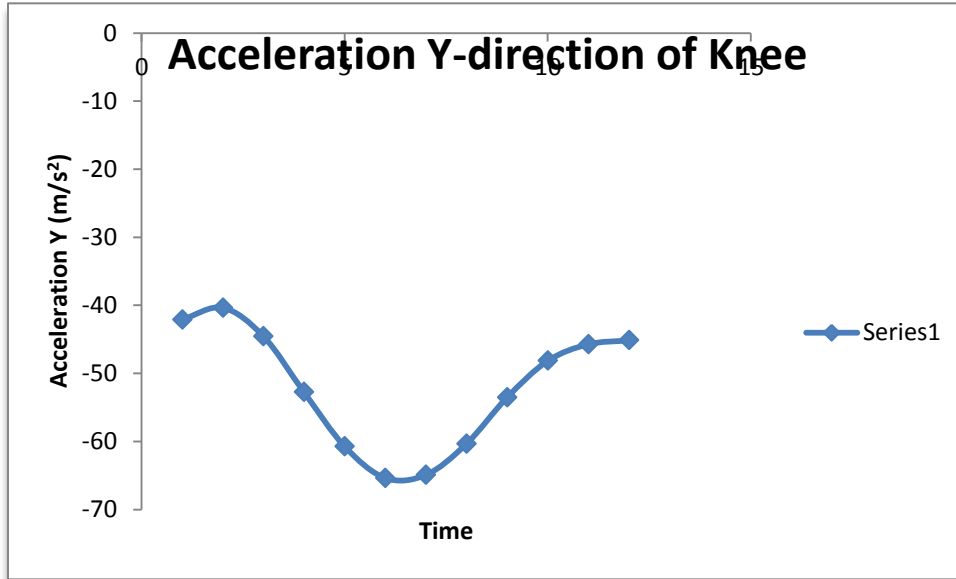


Figure 42: Acceleration in the y-direction of the knee from heel strike to toe off of the gait cycle

Other angles were calculated using the positions of the tracking markers, specifically knee flexion, the angle the shank made with the ground upon impact and ankle flexion. These values were then utilized during the computational bioanalysis of individual subjects. The tabulated results can be viewed in Appendix G. Due to difference in gait forms no average or statistical data could be retrieved from this data. Although foot and knee accelerations were mostly within the same range, no correlation could be made as a population because the running styles were different; therefore factors such as the knee and ankle flexion, as well as the angle of the tibia were also inconsistent. To view the data variability, Figure 43 below displays the spinal rotation of each subject during exaggerated, normal, and restricted test runs plotted against the angle of the tibia upon initial impact.

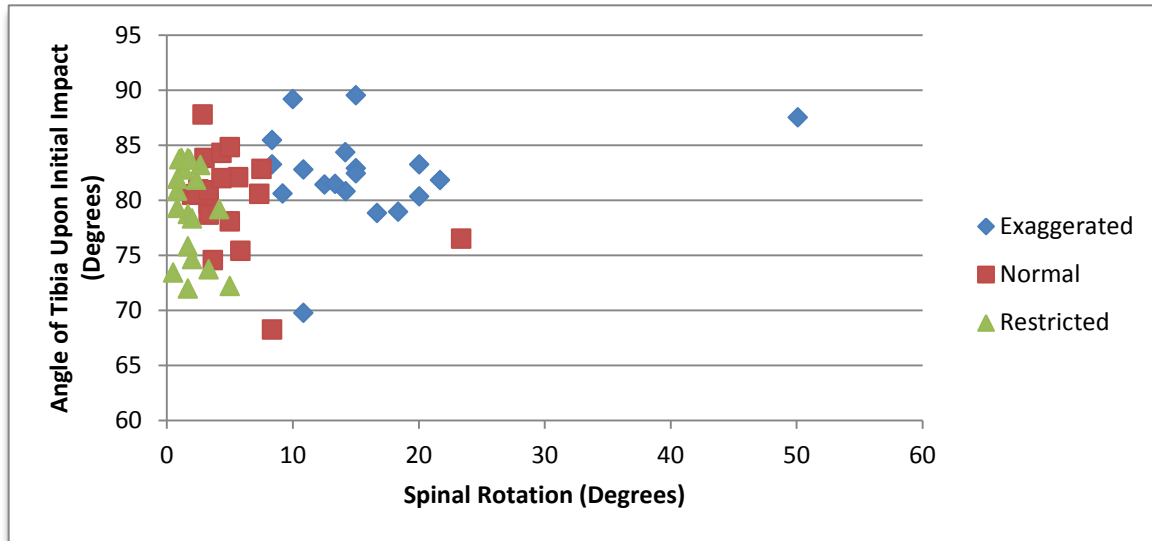


Figure 43: A plot of Spinal rotation vs. the angle of the tibia upon heel strike (initial impact).

This plot displays no discernible correlation between spinal rotation and the angle of the tibia upon impact. The angle of some subjects' shanks increased with increased spinal rotation. Other subjects showed a higher angle during the restricted and even normal running styles. These spinal rotation angles for the different running forms can be found in Appendix F and the Angles of the tibia upon initial impact can be found in Appendix G.

Variations in running forms between test subjects were observed due to the unique innate biomechanics of each individual. This made it challenging to make generalized assumptions about the gait cycle. For example, some runners exhibit heel strike landings while others land on their forefoot. Observations were also made in which a subject's ankle pronated or supinated in the third plane not viewable by the camera configuration. There were no means of accurately accounting for these variations. The foot sensors were placed on the heel insert at the general locations of the center of pressure according to literature. The curves of the voltage readings of the sensors matched the ground reaction force curves seen in literature and preliminary testing. However, the range of the voltage readings varied with each subject due to the unique landing form of each individual. Even when subjects displayed the heel strike form, the center of pressure distribution for each

subject is different; therefore accurate depiction of the impact forces was not achieved because the transducers were not always fully contacted by the heel during heel strike.

The test subjects used for data analysis had changes in their stride length between the restricted, normal, and exaggerated running form. More upper body rotation showed a direct relationship with a longer stride length. There was no correlation between ankle flexion or knee flexion and the magnitude of the joint forces in the ankle or knee, again due to the variation in running styles for each subject. These compressive forces are largely attributed to the center of pressure and where the impact force acts.

Figure 44 below shows spinal rotation vs. stride length for three subjects. As spinal rotation increased, the stride length also increased. This direct relationship was exhibited by most of the subjects.

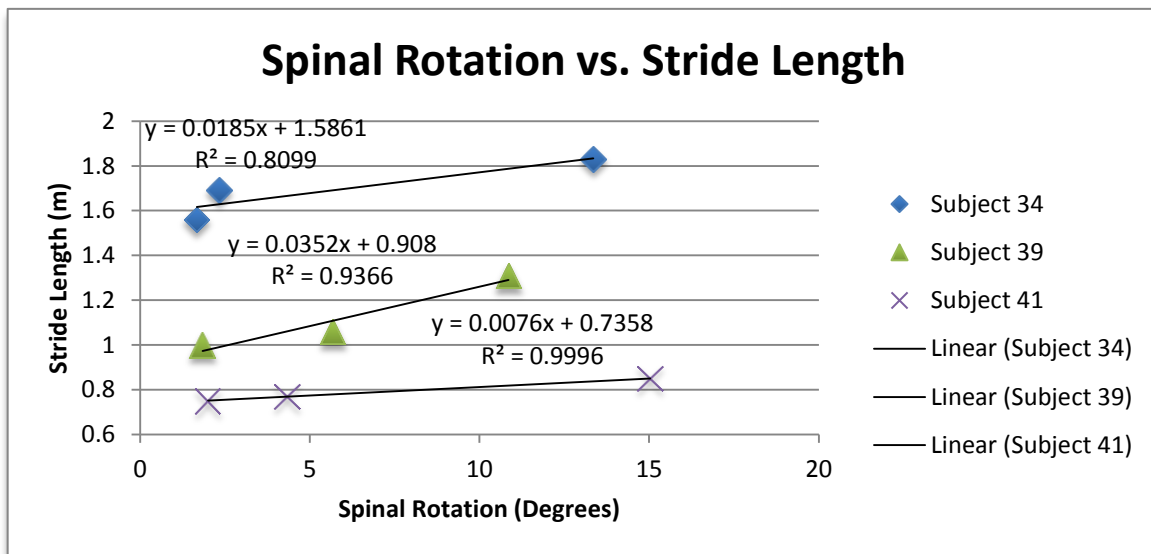


Figure 44: A plot of Spinal Rotation vs. Stride Length

These results can be linked in to the results attained for knee forces and the how hamstring muscles bear the load relative to the joint. The less knee flexion a subject has upon impact, the more the hamstring can bear the load from the knee joint. However, knee flexion is not the only component that determines how force is distributed. Therefore, no correlations were found between knee flexion and ground reaction force or stride length alone. The results for forces in the hamstring and knee joint can be viewed in Appendix I.

Regression analysis was performed to determine the statistical significance between spinal rotation and the length of the subject's stride. The null hypothesis was that the degree of spinal rotation during the gait cycle had no effect on the stride length. A p-value of .00067 was returned. Since $.00067 < .05$, the p-value indicated the null hypothesis could be rejected and that the data was statistically significant.

9.3 Force Plate Analysis

The musculoskeletal models shown in Section 8.3 above were used to calculate values such as the ground reaction force (GRF), the force in the tibialis tendon (F_{ta}), the force in the ankle (F_{ankle}) along with many other forces in other muscles and tendons acting from the foot to the knee. Figure 45 below shows the degree of rotation plotted against the normalized ground reaction force for the four subjects tested on the force plate.

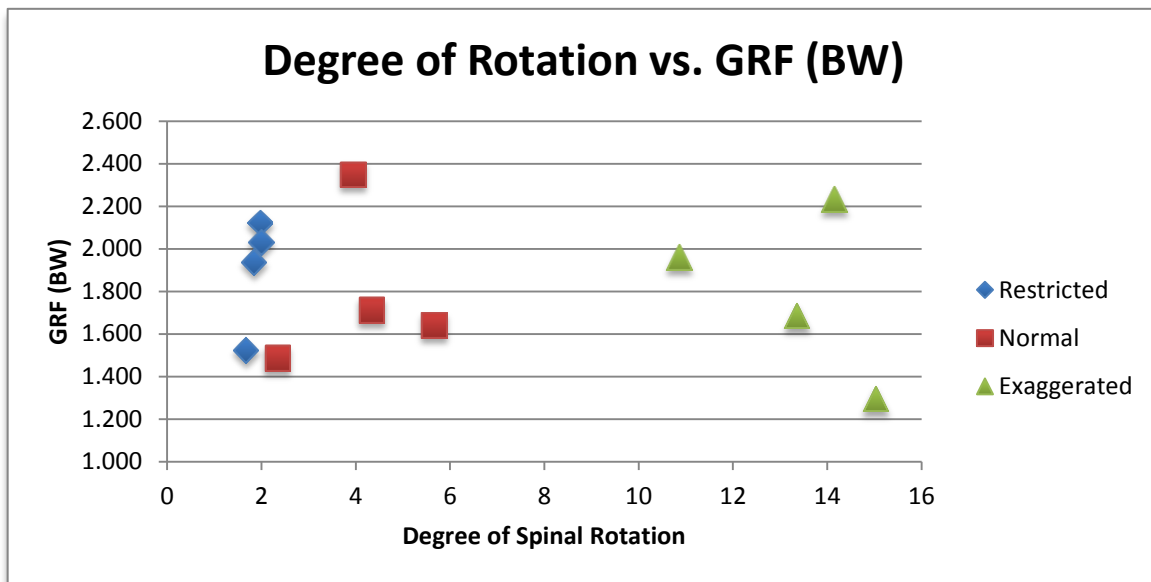


Figure 45: Plot of spinal rotation vs. ground reaction force (body weight) for four subjects tested on force plate.

No correlation was made between spinal rotation and the ground reaction force. The variations in running forms between test subjects' affects force distributions throughout the foot and leg and therefore no single one to one correlation can be made. The group's initial hypothesis that ground reaction forces would decrease with more spinal rotation was rejected.

10. Discussion and Conclusion

This study determined that the hypothesis, which stated that with an increased spinal rotation the impact forces on the lower body would decrease, was not found. Possible future correlations were noticed; however, due to a small group size and variation between subjects, no conclusive theories were supported. For instance, a correlation between stride length and spinal rotation along with reduction in knee compressive force were noticed. Future studies, with a larger test population, could confirm the effect of spinal rotation on a subject's stride length.

For future studies in this area, using a force plate instead of force transducers is recommended along with the use of more cameras to give the tester more tracking points. Although these systems are costly, it is necessary to use the force plate due to the countless variations in landing style and center of pressure from one person to the next. The force plate has a larger surface area allowing for full wireless data collection of the foot. With the use of a force plate it will ensure the subject does not alter their natural running form as well as provide more accurate pressure readings while testing.

With the recommendation of more cameras, not only will the side view be available for analysis of accelerations and velocities of the lower extremities, but other angles (i.e. rear view) could allow for a better understanding of pronation and supination and its effects on the GRF. In order to obtain accurate results for the use of a three dimensional model multiple cameras placed at different angles would have to be used. More cameras also provide tracking of other body parts rather than just the lower limbs. Measurement of the forces on the hip is also an important concept, which should be studied with the effects of spinal rotation and impact forces. Viewing the model in only one plane, the sagittal plane, does not allow for an accurate depiction of the lower body (the ankles, knees, and hip structure), which makes it difficult and very inaccurate to solve for the forces present. Also it is recommended that the camera have faster frame rate and greater resolution than the camera used in this project. With a greater resolution the tracking ability of the camera is more accurate allowing for better tracking of the markers placed on each subject and during video analysis the accuracy of the results will also increase.

11. Manufacturing

Manufacturing and prototyping the device for mass distribution was a key component to the success of the project. The type of materials used for each component is subject to change during the actual manufacturing process in respect to constraints. Another important aspect to manufacturing is the labor force need to build the device.

Specific costs are important to keep in mind; for instance, the metal back plate needed to be rigid and malleable enough to support the function of the device on the back of the participant, understanding of processing machinery is needed. A Pexto Foot Squaring Shear was used to accurately and precisely cut the aluminum back plates; the machine costs approximately \$2500 (Senecal, 1960). To create the necessary slits in the back plate for the Velcro straps a CNC Air Compressed Grinder was used; a CNC Air Compressed Grinder costs approximately \$159.98 (Oll-Tools).

Ideally the expansive growth of a company relies heavily on suitable floor operations with cost effective labor forces. According to Smart Planet, a CNET Professional Brand website, the United States has an average price of manufacturing to individuals per hour of \$19, in Taiwan the average is \$8.36, in Japan the average is \$7.80 and in China the average price of a manufacturer per hour is \$1.36 (CNET). These costs are insightful into how rapidly a company will implode or expand. For the building of this device these prices are helpful because they help a company determine where they would want their device to be built. The lower the cost to make the device the more the company makes after all expenses are paid.

Works Cited

- Baker, R. (2007, September). The history of gait analysis before the advent of modern computers. *Gait & Posture*, 26(3), 331-342.
- Braun, M. (1992). Picturing time: the work of Etienne-Jules Marey (1830-1904).
- CNET. (n.d.). *next-low-cost-manufacturing-center-the-united-states*. Retrieved April 8, 2012, from Smart Planet: <http://www.smartplanet.com/blog/business-brains/next-low-cost-manufacturing-center-the-united-states/15731>
- Drewes, L., McKeon, P., Kerrigan, C., & Hertel, J. (2009). Dorsiflexion deficit during jogging with chronic ankle instability. *Journal of Science and Medicine in Sport*, 685-687.
- Makwana, N., & Liefland, M. (2005). Injuries of the midfoot. *Current Orthopaedics*, 231-243.
- Mazzone, M., & Mccue, T. (2002). Common Conditions of the Achilles Tendon. *American Family Physician*, 1805-1811.
- McDaniel, L. W., Ihlors, M., Haar, C., Jackson, A., & Gaudet, L. (2010). Common Runners/Walkers Foot Injuries. *Contemporary Issues in Education Research*, 69-74.
- Newlin, D. a. (2011). Shin splints 101: explaining shin splints to young runners. *Strategies: A Journal for Physical and Sport Educators*, 10.
- Oll-Tools. (n.d.). *CP7556*. Retrieved April 8, 2012, from OllTools-The Tool for Tools: <http://www.oll-tools.com/product/cp7556/price>
- Perry, J. (1992). *Gait Analysis Normal and Pathological Function*. Thorofare, NJ: SLACK Incorporated.
- Pribut, S. (2010, September 27). *Gait Biomechanics*. Retrieved from <http://www.drpribut.com/sports/spgait.html>
- RadioShack. (2011). Retrieved 10 11, 2011, from RadioShack: <http://www.radioshack.com/product/index.jsp?productId=2062287#>
- Senecal, M. (1960). *Modern Tool LTD*. Retrieved 2011, from Modern Tool: <http://www.moderntoolcatalog.com/catalog/view.php?id=722>

Appendix A

Table 3: Preliminary Function vs. Means tree. This helps to understand the preliminary steps to further understand what we chose as our final design.

Lower Body		Upper Body	
Functions	Means	Functions	Means
Measure reaction forces on foot during gait cycle	-Wireless Transducers -Gel Transducers -Force plate -Balance before initial gait cycle	Measure rotation of the spine around y-axis during gait cycle	-Wireless/Wired transducers -Athletic tape Transducers -Elastic Straps (measures tension) -Under-armor shirt (transducers inside shirt) -Potentiometer
Acquire data	-Accelerometer -Goniometer -Marker transducers (Video) -Force Plate (not a storage device) -Force Transducers	Acquire data from shoulder movement	-Accelerometer -Potentiometer -Goniometer -Marker transducers (Video) -Retractable straps that measure the pull of the shoulders
Transmit data	-Cord/wires -Wireless -Remote Transducers	Record voltage outputs onto a portable storage device	-Analogue device in pole measures y-axis in gait -Different storage devices
Record voltage outputs onto a portable storage device	-Data acquisition box	Attach to back	-Shoulder straps -Velcro -Athletic tape** -Elastic bands -Stainless steel -Aluminum -Rubber -Plastic -Under-armor shirt (transducers inside shirt)
Provide Adjustability	-Retractable cords/wires -Removable insert -Athletic tape**	Provide Adjustability	-Plastic plate with holes/notches -Velcro -Athletic Tape** -Retractable straps that measure the pull

			of the shoulders
Operate on power source	-Battery Powered -Solar Powered -Kinetic Energy -Source Power	Operate on power source	-Battery Powered -Solar Powered -Kinetic Energy -Source Power
Monitor lower limb movement	-Calculations -Video with reflective markers -2-D Video -3-D Video -Still Shots	Monitor upper body movement	--Calculations -Video with reflective markers -2-D Video -3-D Video -Still Shots
Provide comfort	-Light-weight material -Small transducers (unobtrusive) -Transducers evenly distributed	Provide comfort	-Shoulder pads -Padding on plate

Appendix B

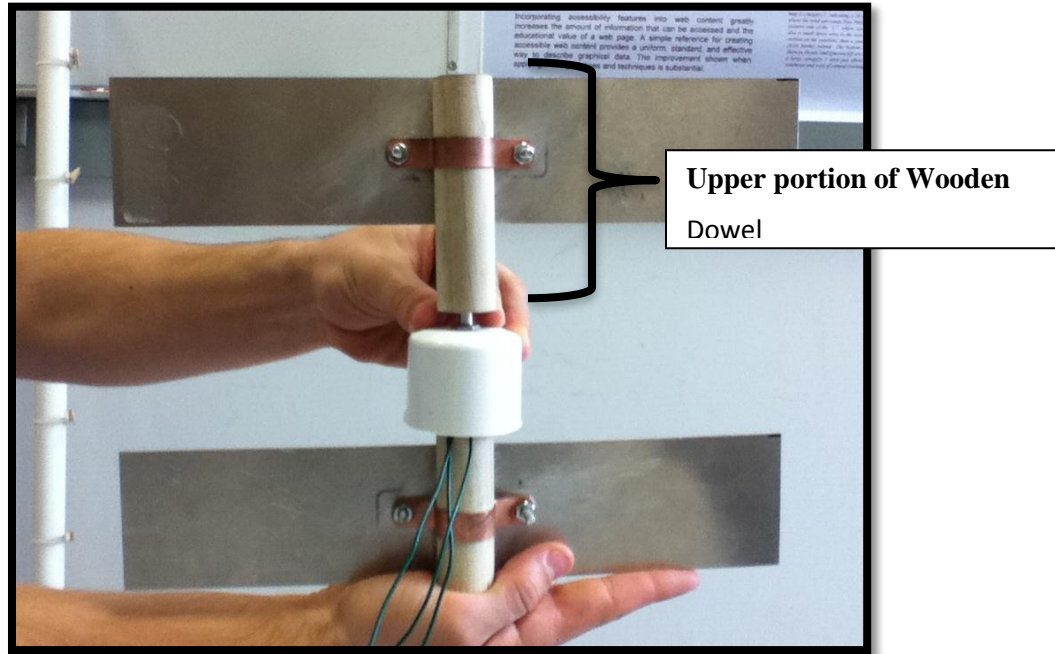


Figure 46: Final Spinal Rotation Design

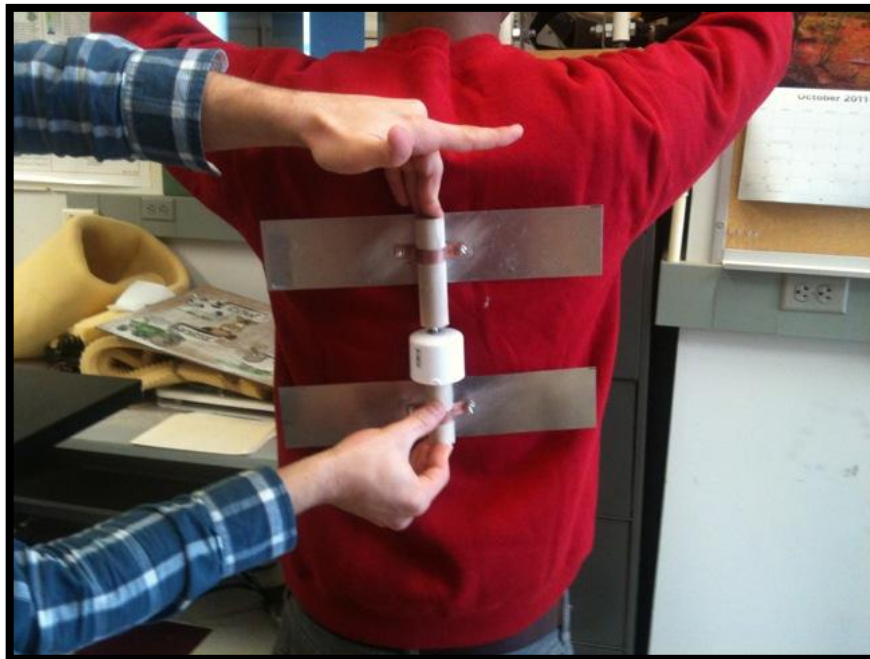


Figure 47: Spinal Rotation Device in Proportion to a Body

Table 4: Outline of Materials for the Spinal Rotation Design

Materials for Spinal Rotation Device	Specifications
Aluminum Metal	Length: 12" Thickness: .032" Height: 2.5"
Wooden Dowel (Upper portion)	Length: 4" Hole in center: .24" Diameter: 1"
Wooden Dowel (Lower portion)	Length: 4" Diameter: 1"
Plastic Cap	Diameter: 2" Center hole: .25"
C-Bracket	Size: .5"
Potentiometer	Note table and figure in Appendix D

Appendix C

Table 5: Specifications of 100K-Ohm Linear-Taper Potentiometer

Model	100K-Ohm Linear-Taper Potentiometer model#:271-092				
Cost	\$3.19				
Specifications	Dimensions <ul style="list-style-type: none"> Length-6mm stem, Width-14mm (.55in), 5/16"- diameter hole, 1-11/16" long X 1/4"-diameter round stem 				
	Power <ul style="list-style-type: none"> Wattage rating of 0.5W. Tolerance 20% 				
	Temperature <table border="1" data-bbox="548 863 1339 953"> <tr> <td>Min Operating Temperature</td> <td>-55 Fahrenheit</td> </tr> <tr> <td>Max Operating Temperature</td> <td>70 Fahrenheit</td> </tr> </table>		Min Operating Temperature	-55 Fahrenheit	Max Operating Temperature
Min Operating Temperature	-55 Fahrenheit				
Max Operating Temperature	70 Fahrenheit				
Supplier	Radioshack				



Figure 48: Shows a 100K-Ohm Linear-Taper Potentiometer

Appendix D

Table 6: Specifications of the FlexiForce force transducer

Model	Tekscan <i>FlexiForce</i> A201
Cost	<ul style="list-style-type: none">• 4-Pack trimmed \$77• 8-Pack trimmed \$140
Dimensions	Length-optional trimmed: <ol style="list-style-type: none">1. 152mm(6in.)2. 102mm(4in.)3. 51mm(2in.), Width-14mm (.55in) Sensing area: 9.53mm (.375) diameter
Supplier	Tekscan



Figure 49: *FlexiForce* Force Transducer used for force measurement

Appendix E

Table 7: Heel strike pressure measurements for force transducers 1 and 2

Subject	Pressure (N/cm ²) Combined Force Transducers 1 and 2		
	Exaggerated	Normal	Restricted
15	1.336	0.256	0.082
16	0.008	0.046	0.037
19	0.010	0.017	0.015
21	0.016	0.025	0.019
22	0.286	0.016	0.977
24	0.037	0.050	0.077
25	0.094	0.039	0.417
26	0.450	1.088	0.546
27	2.519	1.711	2.570
28	0.543	0.817	0.271
29	0.514	0.029	0.052
30	0.021	0.054	0.025
33	0.070	0.044	0.051
34	0.065	0.068	0.055
35	0.288	0.027	0.839
36	0.127	0.060	0.050
37	0.336	0.017	0.015
38	0.155	0.036	0.068
39	0.045	0.054	0.050
40	0.022	0.021	0.030
41	0.041	0.033	0.037

Appendix F

Table 8: Spinal rotation measured in degrees for exaggerated, normal, and restricted rotation.

Subject	Exaggerated (Degrees)	Normal (Degrees)	Restricted (Degrees)
15	14.19	5.01	0.83
16	9.18	2.67	0.83
19	50.10	23.38	3.34
21	9.18	3.34	0.50
22	15.03	8.35	2.33
24	18.37	3.34	2.00
25	16.70	3.67	1.33
26	20.04	3.00	1.67
27	14.19	2.00	1.67
28	8.35	7.51	2.67
29	12.52	2.50	0.83
30	10.02	2.67	1.33
33	8.35	4.34	1.16
34	13.36	2.33	1.67
35	15.03	5.84	4.17
36	20.04	5.01	1.00
37	21.71	7.34	5.01
38	10.02	3.34	1.67
39	10.85	5.67	1.83
40	10.85	2.83	0.83
41	15.03	4.34	2.00
Mean	15.40	5.21	1.83
Standard Deviation	9.14	4.66	1.17

Appendix G

Table 9: Compilation of various parameters from video analysis.

Subject	Calculated Parameter	Normal	Exaggerated	Restricted
15	Angle of Tibia (Degrees)	80.78	78.06	80.84
	Stride Length (m)	1.08	1.28	0.85
	Spinal rotation (Degrees)	14.2	5.01	0.84
	Velocity (m/s)	5	4.52	4
Subject	Calculated Parameter	Normal	Exaggerated	Restricted
19	Angle of Tibia (Degrees)	87.49	76.5	73.71
	Stride Length (m)	1.15	1.54	1.02
	Spinal rotation (Degrees)	50.11	23.38	3.34
	Velocity (m/s)	5.45	5.33	5.11
Subject	Calculated Parameter	Normal	Exaggerated	Restricted
21	Angle of Tibia (Degrees)	80.59	79.69	73.41
	Stride Length (m)	1.51	1.61	1.28
	Spinal rotation (Degrees)	9.19	3.34	0.5
	Velocity (m/s)	4.89	5.22	4.8
Subject	Calculated Parameter	Normal	Exaggerated	Restricted
22	Angle of Tibia (Degrees)	82.87	68.25	81.83
	Stride Length (m)	1.28	1.46	1.22
	Spinal rotation (Degrees)	15.03	8.35	2.34
	Velocity (m/s)	5.33	4.62	4.53
Subject	Calculated Parameter	Normal	Exaggerated	Restricted
24	Angle of Tibia (Degrees)	78.82	74.55	82.78
	Stride Length (m)	1.14	1.33	1.11
	Spinal rotation (Degrees)	18.37	3.34	2
	Velocity (m/s)	4.8	4.36	3.58
Subject	Calculated Parameter	Normal	Exaggerated	Restricted
25	Angle of Tibia (Degrees)	78.82	74.55	82.78
	Stride Length (m)	1.36	1.43	1.16

	Spinal rotation (Degrees)	16.7	3.65	1.34
	Velocity (m/s)	5.45	5	4.71
Subject	Calculated Parameter	Normal	Exaggerated	Restricted
26	Angle of Tibia (Degrees)	83.22	83.81	78.73
	Stride Length (m)	1.04	1.1	0.89
	Spinal rotation (Degrees)	20.04	3.01	1.67
	Velocity (m/s)	4.44	4.06	4.29
Subject	Calculated Parameter	Normal	Exaggerated	Restricted
27	Angle of Tibia (Degrees)	84.34	80.48	83.77
	Stride Length (m)	0.87	0.99	0.86
	Spinal rotation (Degrees)	14.19	2	1.67
	Velocity (m/s)	3.24	4.13	3.58
Subject	Calculated Parameter	Normal	Exaggerated	Restricted
28	Angle of Tibia (Degrees)	83.24	82.82	83.17
	Stride Length (m)	0.97	1.1	1
	Spinal rotation (Degrees)	8.35	7.52	2.67
	Velocity (m/s)	4.29	4.21	4.53
Subject	Calculated Parameter	Normal	Exaggerated	Restricted
29	Angle of Tibia (Degrees)	81.41	80.98	79.28
	Stride Length (m)	1.02	1.08	0.89
	Spinal rotation (Degrees)	12.53	2.51	0.84
	Velocity (m/s)	3.63	4.13	3.69
Subject	Calculated Parameter	Normal	Exaggerated	Restricted
33	Angle of Tibia (Degrees)	85.43	84.29	83.82
	Stride Length (m)	0.98	1.04	0.88
	Spinal rotation (Degrees)	8.35	4.34	1.17
	Velocity (m/s)	2.96	3.33	3
Subject	Calculated Parameter	Normal	Exaggerated	Restricted
34	Angle of Tibia (Degrees)	81.47	80.54	75.79
	Stride Length (m)	1.69	1.83	1.56
	Spinal rotation (Degrees)	13.36	2.34	1.67

	Velocity (m/s)	4.21	4.36	4.21
Subject	Calculated Parameter	Normal	Exaggerated	Restricted
35	Angle of Tibia (Degrees)	89.5	75.38	79.15
	Stride Length (m)	1.27	1.59	1.21
	Spinal rotation (Degrees)	15.03	5.85	4.18
	Velocity (m/s)	4.89	4.29	4
Subject	Calculated Parameter	Normal	Exaggerated	Restricted
36	Angle of Tibia (Degrees)	80.34	84.79	83.69
	Stride Length (m)	1.01	1.03	1
	Spinal rotation (Degrees)	20.04	5.01	1
	Velocity (m/s)	4.07	3.24	3.87
Subject	Calculated Parameter	Normal	Exaggerated	Restricted
37	Angle of Tibia (Degrees)	81.82	80.56	72.19
	Stride Length (m)	1.29	1.43	1.22
	Spinal rotation (Degrees)	21.71	7.35	5.01
	Velocity (m/s)	4.8	4.36	4.53

Subject	Calculated Parameter	Normal	Exaggerated	Restricted
38	Angle of Tibia (Degrees)	89.15	80.87	71.97
	Stride Length (m)	1.65	1.82	1.45
	Spinal rotation (Degrees)	10.02	3.34	1.67
	Velocity (m/s)	4.14	5.22	5.33
Subject	Calculated Parameter	Normal	Exaggerated	Restricted
39	Angle of Tibia (Degrees)	82.77	82.06	83.66
	Stride Length (m)	1.06	1.31	1
	Spinal rotation (Degrees)	10.86	5.68	1.84
	Velocity (m/s)	3.64	3.38	3.69
Subject	Calculated Parameter	Normal	Exaggerated	Restricted
40	Angle of Tibia (Degrees)	69.74	87.76	81.92
	Stride Length (m)	1.41	1.55	1.39
	Spinal rotation (Degrees)	10.86	2.84	0.84

	Velocity (m/s)	4.89	4.44	4.89
Subject	Calculated Parameter	Normal	Exaggerated	Restricted
41	Angle of Tibia (Degrees)	82.42	81.99	78.33
	Stride Length (m)	0.77	0.85	0.75
	Spinal rotation (Degrees)	15.03	4.34	2
	Velocity (m/s)	3.16	3.24	3.24

Appendix H

Table 10: Angular Accelerations of the tibia for the three running forms

	Exaggerated	Normal	Restricted
Subject	Angular Acceleration of Tibia [rad/sec ²]	Angular Acceleration of Tibia [rad/sec ²]	Angular Acceleration of Tibia [rad/sec ²]
15	139.44	115.77	86.58
19	136.6	23.99	110.95
21	89.14	59.32	50.76
22	124.55	65.5	69.85
24	102.26	62.3	92.8
25	117.17	69.05	107.64
26	171.69	94.45	30.47
27	155.75	98.45	77.62
28	597.54	64.99	48.76
29	72.68	77.46	69.99
33	41.53	52.65	76.97
34	170.11	113.95	96.45
35	169.03	141.6	95.89
36	94.17	120.38	39.69
37	101.95	65.64	43.46
38	72.36	65.5	77.41
39	125.93	88.87	77.47
40	209.66	204.68	144.12
41	92.6	38.49	86.29

Appendix I

Table 11: Compilation of the forces experienced in lower leg using musculoskeletal models and computational bioanalysis.

Restricted Rotation (°)	GRF (BW)	Fta (BW)	Fankle (BW)	Fach (BW)	Fknee (BW)	Fham (BW)	Fpt (BW)	Stance Time (s)
1.97	2.122	5.674	7.795	4.592	11.606	7.364	6.213	0.232
1.67	1.522	3.678	4.780	2.845	6.420	4.971	3.166	0.326
2	2.032	6.617	8.746	4.473	8.315	7.859	2.836	0.288
1.84	1.937	4.486	5.396	3.089	12.315	7.870	6.761	0.274
Average	1.903	5.114	6.680	3.750	9.664	7.016	4.744	0.280
St.dev.	0.265	1.295	1.895	0.911	2.777	1.383	2.030	0.039

Normal Rotation (°)	GRF (BW)	Fta (BW)	Fankle (BW)	Fach (BW)	Fknee (BW)	Fham (BW)	Fpt (BW)	Stance Time (s)
3.95	2.35	8.54	12.63	6.96	12.48	8.72	5.70	0.242
2.34	1.48	1.71	4.07	5.36	3.25	9.07	5.80	5.004
4.34	1.71	5.21	7.56	4.39	11.96	7.72	5.89	0.276
5.67	1.64	3.26	4.10	2.54	7.12	4.79	3.95	0.268
Average	1.795	4.680	7.091	4.813	8.701	7.573	5.335	1.448
St.dev.	0.380	2.946	4.041	1.849	4.361	1.944	0.926	2.371

Exaggerated Rotation (°)	GRF (BW)	Fta (BW)	Fankle (BW)	Fach (BW)	Fknee (BW)	Fham (BW)	Fpt (BW)	Stance Time (s)
14.15	2.23	6.88	9.83	5.62	11.92	8.13	5.86	0.242
13.36	1.68	3.35	3.65	2.16	4.73	4.33	2.40	0.300
15.03	1.30	4.46	6.15	3.22	6.60	5.67	2.39	0.296
10.86	1.96	3.24	4.09	2.15	5.49	4.63	2.30	0.304
Average	1.793	4.481	5.931	3.288	7.186	5.689	3.235	0.286
St.dev.	0.400	1.693	2.822	1.635	3.250	1.724	1.749	0.029